Quark-Quark and Quark-Nucleon Potential Model Extended-soft-core Meson-exchange Interactions

Th.A. Rijken

Institute of Mathematics, Astrophysics, and Particle Physics
Radboud University, Nijmegen, The Netherlands

Y. Yamamoto

Nishina Center for Accelerator-Based Science,
Institute for Physical and Chemical Research (RIKEN),
Wako, Saitama, 351-0198, Japan.

Abstract

The Quark-quark (QQ) and Quark-nucleon (QN) interactions in this paper are derived from the Extended-soft-core (ESC) interactions. The meson-quark-quark (MQQ) vertices are determined in the framework of the constituent quark-model (CQM). These vertices are such that upon folding with the ground-state baryonic quark wave functions the one-boson-exchange amplitudes for baryon-baryon (BB), and in particularly for nucleon-nucleon (NN), are reproduced. This opens the attractive possibility to define meson-quark interactions at the quark-level which are directly related to the interactions at the baryon-level. The latter have been determined by the baryon-baryon data. Application of these "realistic" quark-quark interactions in the quark-matter phase is presumably of relevance for the description of highly condensed matter, as e.g. neutron-star matter.

These quark-quark potentials consist of local- and non-local-potentials due to (i) One-boson-exchanges (OBE), which are the members of nonets of pseudo-scalar-, vector-, scalar-, and axial-mesons, (ii) Diffractive exchanges, (iii) Two pseudo-scalar exchange (PS-PS), and (iv) Meson-Pair-exchange (MPE). Both the OBE- and Pair-vertices are regulated by gaussian form factors producing potentials with a soft behavior near the origin. The assignment of the cut-off masses for the BBM-vertices is dependent on the SU(3)-classification of the exchanged mesons for OBE, and a similar scheme for MPE. The model is presented in the framework of the Kadyshevski formalism, which has the advantage that in momentum space fully relativistic potentials can be used in principle.

Like previous ESC models, the recent ESC16 describes nucleon-nucleon (NN), hyperon-nucleon (YN), and hyperon-hyperon (YY) in a unified way using broken SU(3)-symmetry. Novel ingredients are the inclusion of (i) the axial-vector meson potentials, (ii) a zero in the scalar- and axial-vector meson form factors. These innovations made it possible to keep the parameters of the model closely to the predictions of the quark-antiquark pair creation (QPC) model, with a dominance of the $^3P_0$-pair creation. This is also the case for the flavor SU(3) $F/(F+D)$-ratio's. In this QPC-model to the couplings in the framework of the CQM the mesons are coupled directly to the quarks. Therefore, it is most natural to consider meson-exchange on the quark-level as the basis for the meson-exchange BB-potentials. In this paper we derive the QQ- and QN-interactions for the two-quark and the quark-nucleon channels of the basic isodoublet i.e. U,D quarks: (i) UU-, UD-, and DD-channels, and (ii) UP-, UN- and DN-channels, with P=proton, N=neutron. Applications of these potentials can be made for the mixed nuclear and quark matter, which probably occurs for example inside neutron stars.

I. INTRODUCTION

The Quark-quark and Quark-nucleon/baryon interactions in this paper are derived from the Extended-soft-core (ESC) interactions. In [1, 2] we have determined the meson-quark-quark (QQM) vertices in the framework of the constituent quark-model (CQM) [3–6]. These QQM-vertices are such that upon folding with the effective ground-state baryonic harmonic oscillator quark wave functions, the one-boson-exchange amplitudes for nucleon-nucleon (NN) are reproduced. This opens the attractive possibility to define meson-quark interactions at the quark-level which are directly related to the interactions at the baryon-level. The latter have been determined by the baryon-baryon data. These "unified" quark-quark and quark-nucleon/baryon interactions can be applied to the nucleon-quark mixed-matter phase, which is relevant for the description of highly condensed matter, as e.g. neutron-star matter.

In QCD two non-perturbative effects occur: (i) confinement and (ii) chiral symmetry breaking. The $SU(3)_L$x$SU(3)_R$ chiral symmetry is spontaneously broken to an $SU(3)_v$ symmetry at some scale $\Lambda_{\chi SB} \approx 1$ GeV. Below this scale there is an octet of pseudoscalar Goldstone-bosons: (π, K, η). The confinement scale $\Lambda_{QCD} \approx 100 - 330$ MeV. The complex QCD-vacuum structure can be described as an BPST instanton/anti-instanton liquid giving the valence quarks a dynamical or constituent effective mass $\approx M_N/3$ [7, 8]. This corresponds to the CQM [6], which is the basis for the quark-quark and quark-nucleon interactions proposed in this paper.

The QQ-interactions in this paper consist of local- and non-local-potentials due to (i) One-boson-exchanges (OBE), which are the members of nonets of pseudo-scalar-, vector-, scalar-, and axial-mesons, (ii) Diffractive exchanges, (iii) Two pseudo-scalar exchange (PS-PS), and (iv) Meson-Pair-exchange (MPE). Both the OBE- and Pair-vertices are regulated by gaussian form factors producing potentials with a soft behavior near the origin. The assignment of the cut-off masses for the BBM-vertices is dependent on the SU(3)-classification of the exchanged mesons for OBE, and a similar scheme for MPE.

The ESC-models in general, and so also the recent version ESC16 [9–11], describe nucleon-nucleon (NN) and hyperon-nucleon (YN) in a unified way using broken SU(3)-symmetry. Novel ingredients in ESC16 are the inclusion of (i) the axial-vector meson potentials, (ii) a zero in the scalar- and axial-vector meson form factors. These innovations made it possible for the first time to keep the parameters of the model closely to the predictions of the $^3P_0$ quark-antiquark creation (QPC) model [3, 5]. This is also the case for the $F/(F+D)$-ratio's. The application of the QPC model to the couplings was executed in the framework of the constituent quark-model. Therefore, it is most natural to consider meson-exchange on the quark-level. In this paper we derive the QQ-interactions for the two-quark channels of the basic triplet i.e. U,D, and S quarks: (i) UU-, UD-, and DD-, (ii) US- and DS-, (iii) SS-channels.

The BBM-vertices are described by coupling constants and form factors, which correspond to the Regge residues at high energies [12]. The form factors are taken to be of the gaussian-type, like the residue functions in many Regge-pole models for high energy scattering. Although the gaussian quark wave functions lead to gaussian type of form factors, also in (nonrelativistic) quark models (QM's) a gaussian behavior of the form factors is most natural, because the mesons are Reggeons. These quark-quark-meson form factors evidently guarantee a soft behavior of the potentials in configuration space at small distances.

In the ESC models, see *e.g.* [13], the assignment of the cut-off parameters in the form factors is made for the individual baryon-baryon-meson (BBM) vertices, constrained by broken $SU(3)$-symmetry. The same scheme we follow here for the QQM-vertices.

Confinement is related to the infrared behavior of QCD. This plays an important role when the quarks are not close together. In quark-matter the quark-density is high and therefore the quark-quark interaction is dominantly of short range. So, the infrared behavior can be ignored, being the justification for the use of the same formalism for quarks in (dense) quark matter as for nucleons in nuclear matter.

The contents of this paper are as follows. In section II we review some facts about the "constituents quarks", within the context of spontaneously broken chiral symmetry (Nambu-Goldstone), and the complex structure of the QCD vacuum. In section III the relation between the ESC BBM-couplings and the QQM-couplings is argued for the CQM. In section IV we present the Kadyshevsky formalism [14–17] for baryon-baryon channels and the three-dimensional "quasi-potential equation. From this a in section V a Thompson-type relativistic Lippmann-Schwinger is derived using a standard [14] on-energy-shell version of the Kadyshevsky equation. In section VI the Lippmann-Schwinger and the Bethe-Goldstone equations are given. In section VII the ESC meson-quark-quark and meson-nucleon-nucleon interaction Hamiltonians are displayed, both for the QQM/NNM-vertices as well as for the pair-vertices QQMM/NNMM. Here also the meson-pair interaction Hamiltonians are given in the context of $SU(3)$. Expressions for the meson-pair-exchange (MPE) graphs are given, again in an immediately programmable form. In section VIII we describe the $S = 0, -1, -2$ QQ-channels on the isospin (i) and hypercharge (y) and particle basis. Here also the SU(3)-structure of the QQM/NNM-couplings are given both in the 3×3-matrix and cartesian-nonet description. Outlined is the (numerical) evaluation of the couplings which occur in the OBE- and TME-diagrams. In section IX the same is done for the meson-pair couplings and MPE-diagrams. Here also the gaussian form factors are mentioned. In section X the connection between the QQM- and BBM-couplings are listed. In section XI the one-gluon-exchange (OGE) and confining potentials are described. In section XII the SU(3) Nambu-Jona-Lasinio (NJL) form of the instanton potential is worked out. with the ESC-couplings is discussed. In section XIII the simultaneous $NN \oplus YN$ fitting procedure of the meson-exchange parameters is briefly reviewed, and the results for the coupling constants and $F/(F+D)$-ratios for OBE and MPE are given. Furthermore, results for the QQ-, QN-, and NN-phase-shifts are given. *This is only meant for a comparison of the strength of the QQ- and QN-interactions and the NN-interactions.* In section XIV a summary and an outlook is given.
In Appendix A the the Bethe-Goldstone-Kadyshevsky equation and the correspondent G-matrix are described. In Appendix B a simple model for the relation between the meson-couplings using the Fierz-transformation is described. In Appendix C the complete meson-quark vertices in Pauli-spinor space are given. In Appendix D the one-boson-exchange quark-quark potentials in momentum- and configuration-space are given for the vertices which also occur at the baryon-level. In Appendix E the additional quark-quark potentials are given, which are due to the extra meson-vertices at the quark-level. Next we included some miscellaneous topics: In Appendix F discusses the inclusion of the Z-graphs in the MPE-ineteraction is implicit.

II. CONSTITUENT QUARKS AND INSTANTONS

The spectra of the nucleons, Δ resonances and the hyperons Λ, Σ, Ξ are descibed in detail by the Glozman-Riska model [18]. This is a modern version of the CQM [4] based on the Nambu-Goldstone spontaneous chiral-symmetry breaking (SCSB) with quarks interacting by the exchange of the $SU(3)_F$ octet of pseudoscalar mesons [18]. The pseudoscalar octet are the Nambu-Goldstone bosons (NGB's) associated with the hidden (approximate) chiral symmetry of QCD. The confining potential is chosen to be harmonic, as is rather common in constituent quark models. In line with this, we used harmonic wave functions in the derivation of the connection between the meson-baryon and meson-quark couplings [1]. The η', which is dominantly an SU(3) singlet, decouples from the original nonet because of the U(1) anomaly [19, 20]. According to the two-scale picture of Manohar and Georgi [6] the effective degrees for the 3-flavor QCD at distances beyond that of SCSB ($\Lambda_{\chi SB}^{-1} \approx 0.2 - 0.3$ fm), but within that of the confinement scale $\Lambda_{QCD}^{-1} \approx 1$ fm, should be the constituent quarks and chiral meson fields. The two non-perturbative effects in QCD are confinement and chiral symmetry breaking. The $SU(3)_L \otimes SU(3)_R$ chiral symmetry is sponteneously broken to an $SU(3)_v$ symmetry at a scale

$\Lambda_{\chi SB} \approx 1$ GeV. The confinement scale is $\Lambda_{QCD} \approx 100 - 300$ MeV, which roughly corresponds to the baryon radius ≈ 1 fm. Due to the complex structure of the QCD vacuum, which can be understood as a liquid of BPST instantons and anti-instantons [7, 8, 21, 22], the valence quarks acquire a dynamical or constituent mass [6, 8, 19, 22, 23]. The interaction between the instanton and the anti-instanton is a dipole-interaction [24], similar to ordinary molecules: weak attraction at large distances and strong repulsion at small ones. With the empirical value of the gluon condensate [25] as input the instanton density and radius become [24] $n_c = 8 \cdot 10^{-4}$ GeV^{-4}, and $\rho_c = (600 \text{ MeV})^{-1} \approx 0.3$ fm respectively. Also, with these parameters the non-perturbative vacuum expectation value for the quark fields is $\langle vac|\bar{\psi}\psi|vac\rangle \approx -10^{-2}$ GeV^3 and the quark effective (u,d) masses $\approx$ 200 MeV, i.e. much larger than the almost massless "current masses". In the calculation of light quarks in the instanton vacuum [8] the effective quark mass $m_Q(p = 0) = 345$ MeV was calculated, which is remarkably close to the constituent mass $M_N/3$.

Very notable is the role of the instantons for the light meson spectrum. They give a non-perturbative gluonic interaction between quarks in QCD. For example the instanton-induced interaction, as proposed by 't Hooft [20], generates at low momenta the constituent quark mass [8], i.e. breaks chiral symmetry. This interaction supplies a strong attractive attraction in the pseudoscalar-isovector quark-antiquark system - pions -, which makes them anomalously light, with zero mass in the chiral limit. This is the mechanism by which the pions, being quark-antiquark bound states, appear as Nambu-Goldstone bosons of the SCSB symmetry. This strongly attractive interaction is absent in vector mesons [26, 27], making the masses of the vector mesons $\approx 2m_Q$ in accordance with $m_\rho \approx m_\omega \approx 2m_Q$. Since $\alpha_s \approx 0.3$ the one-gluon-exchage (OGE) is weak, and therefore the $\pi - \rho$ mass splitting is not due to the perturbative color-magnetic spin-spin interaction between the quark and antiquark [26]. Besides explaining the $\pi - \rho$ mass difference, the 't Hooft interaction also in a natural way solves the $U_A(1)$ problem, and gives the reason why the η' is heavy, as distinct to the NGB pseudoscalar octet.

The 't Hooft four-fermion instanton mediated interaction for the light flavor doublet $\psi = (u, d)$, in the form of a generalized Nambu-Jona-Lasinio Lagrangian [28], is

$$\mathcal{L}_I = G_I \left[(\bar{\psi}\psi)^2 - (\bar{\psi}\gamma_5\tau\psi)^2 - (\bar{\psi}\tau\psi)^2 + (\bar{\psi}\gamma_5\psi)^2\right]. \tag{2.1}$$

Here, the strength of the interaction G_I and the ultraviolet cut-off scale $1/r_0$ are related in the instanton liquid model [29]. In this model $G_I = \lambda_{ud}/4 = 2n_+/\langle\bar{\psi}\psi\rangle)^2$. In [30] Glozman and Varga show that the t-channel iteration of the instanton interaction (2.1) leads to isoscalar and isovector pseudoscalar and scalar exchange quark-quark potentials. Since these potentials are already included in our model, the four-fermion instanton interaction does not lead to extra potentials.

In this paper we extend the meson-exchange between quarks by proposing to include, besides the pseudoscalar, all meson nonets: vector, axial-vector, scalar etc. *Since all these meson nonets can be considered as quark-antiquark bound states, there is no reason to exclude any of these mesons from the quark-quark interactions. Furthermore, our preferred value for the constituent quark mass has a solid basis in the instanton-liquid model of the QCD vacuum.*

III. ESC-POTENTIALS AND THE CONSTITUENT QUARK-MODEL

The fitted ESC16-couplings and the QPC-couplings agree very well as shown in [9]. In particular, the SU(6)-breaking improves the agreement significantly. The calculation of Table II in Ref. [9] uses the constituent quark model (CQM) in the SU(6)-version of [3]. In Appendix B a simple model for the quark-antiquark creation process exhibits the main features of the meson-coupling pattern in the ESC models. Since such calculations implicity uses the direct coupling of the mesons to the quarks, it defines the QQM-vertex. Then, OBE-potentials can be derived by folding meson-exchange with the quark wave functions of the baryons. Prescribed by the Dirac-structure, at the baryon level the vertices

have in Pauli-spinor space the $1/M_B$-expansion

$$\bar{u}(p',s')\Gamma u(p,s) = \chi'^{\dagger}_{s'}\left\{\Gamma_{bb} + \Gamma_{bs}\frac{\boldsymbol{\sigma}\cdot\mathbf{p}}{E+M} - \frac{\boldsymbol{\sigma}\cdot\mathbf{p}'}{E'+M'}\Gamma_{sb} - \frac{\boldsymbol{\sigma}\cdot\mathbf{p}}{E+M}\Gamma_{ss}\frac{\boldsymbol{\sigma}\cdot\mathbf{p}'}{E'+M'}\Gamma_{sb}\right\}\chi_s$$
$$\equiv \sum_l c^{(l)}_{BB}\left[\chi'^{\dagger}_{s'}O_l(\mathbf{p}',\mathbf{p})\,\chi_s\right](\sqrt{M'M})^{\alpha_l}\ \ (l = bb, bs, sb, ss). \tag{3.1}$$

This expansion is general and does not depend on the internal structure of the baryon. A similar expansion can be made on the quark-level, but now with quark masses m_Q and coefficients $c^{(l)}_{QQ}$. It appears that in the CQM, i.e. $m_Q = M_B/3$, the QQM-vertices can be chosen such that the ratio's $c^{(l)}_{QQ}/c^{(l)}_{BB}$ are constant for each type of meson [1] Then, these coefficients can be made equal by (i) scaling the couplings, (ii) introducing some extra couplings at the quark level, and (iii) introducing a QQM gaussian form factor. Ipso facto this defines a meson-exchange quark-quark interaction.

IV. KADYSHEVSKY EQUATIONS IN MOMENTUM SPACE

We envisage the interaction between two (constituent) quarks in a dense medium of baryons and/or quarks. In such a condition it is appropriate to consider the QQ-correlations in the G-matrix formalism in the setting of the Bethe-Goldstone equations [31, 32]. To make contact with the 3-dimensional potental formalism we employ the Kadyshevsky formalism [14].

A. Relativistic Two-Body Equation

We consider the quark-quark and quark-nucleon baryon-baryon reactions

$$Q_a(p_a,s_a) + Q_b(p_b,s_b) \to Q'_a(p'_a,s'_a) + Q'_b(p'_b,s'_b), \tag{4.1a}$$
$$Q_a(p_a,s_a) + N_b(p_b,s_b) \to Q'_a(p'_a,s'_a) + N'_b(p'_b,s'_b). \tag{4.1b}$$

The set-up of the scattering formalism for baryon-baryon interactios is given in [9–11] and is given here for completeness.
Introducing, as usual, the total and relative four-momentum for the initial and final state

$$\begin{array}{ll} P = p_a + p_b & ,\ P' = p'_a + p'_b\,, \\ p = \frac{1}{2}(p_a - p_b) & ,\ p' = \frac{1}{2}(p'_a - p'_b)\,, \end{array} \tag{4.2}$$

We use in the following the notation $P_0 \equiv W$ and $P'_0 \equiv W'$. In the Kadyshevsky formulation one introduces four-momenta spurions, making formally four-momentum conservation at the vertices. These are described by quasi-particle states $|\kappa\rangle$, normalized by $\langle\kappa'|\kappa\rangle = \delta(\kappa'-\kappa)$. Then the four-momentum of such a state is κn^μ, where n^μ is time-like with $n^0 > 0$ and $n^2 = 1$. So, we consider the process in (4.1) with non-conservation of the four-momentum, i.e. off-momentum-shell. This off-shellness is given by

$$p_a + p_b + \kappa n = p'_a + p'_b + \kappa' n \tag{4.3}$$

In the following, the on-mass-shell momenta for the initial and final states are denoted respectively by p_i and p_f. So, $p_{i0} = E(\mathbf{p}_i) = \sqrt{\mathbf{p}_i^2 + M^2}$ and $p_{f0} = E(\mathbf{p}_f) = \sqrt{\mathbf{p}_f^2 + M^2}$.

In the Kadyshevsky-formulation the particles are on-mass-shell in the Green-functions. The on-mass-shell propagator $S^{(\pm)}(p)$ of a spin-0 particle can be written as

$$S^{(\pm)}(p) = \delta_\pm(p^2 - M^2) = \frac{1}{2E(\mathbf{p})}\delta\left(p_0 \mp E(\mathbf{p})\right)\,, \tag{4.4}$$

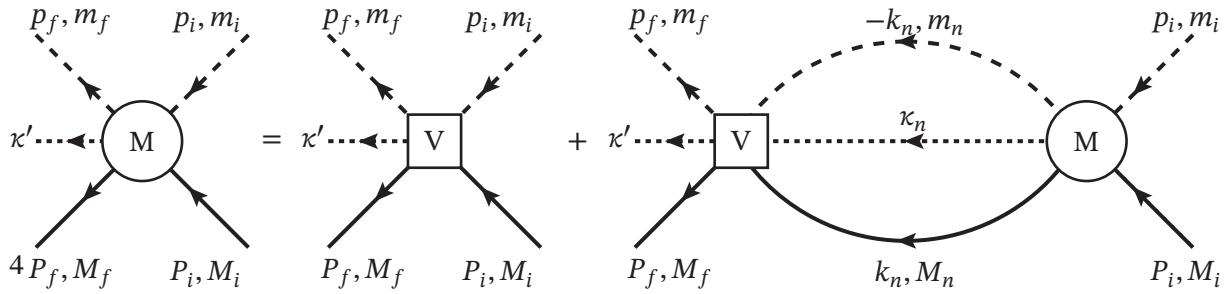

FIG. 1: *M-matrix: Kadyshevsky-Integral Equation*

with $\delta_\pm(p^2 - M^2) \equiv \theta(\pm p^0)\delta(p^2 - M^2)$. The propagator $G_0(\kappa)$ for the quasi-particles is given by [15]

$$G_0(\kappa) = (1/2\pi)\,[1/(\kappa - i\delta)]\ . \tag{4.5}$$

In the Kadyshevsky-formalism the rules for the computation of the off-shell S-matrix, denoted by R, corresponding to the analogs of the Feynman graphs are given [15–17]. [1] We introduce the usual M-matrix by

$$\begin{aligned} R_{\kappa',\kappa}(p'_a, p'_b; p_a, p_b) \ &= \ \delta(\kappa' - \kappa)\delta(p'_a - p_a)\delta(p'_b - p_b) - (2\pi)^4 i\delta^4(\kappa' n + p'_a + p'_b - p_a - p_b - \kappa n)\cdot \\ &\quad \times M_{\kappa',\kappa}(p'_a, p'_b; p_a, p_b)\ . \end{aligned} \tag{4.6}$$

Notice that the S-matrix is given by $R_{0,0}$ [15]. We also observe that

$$\delta(\kappa' - \kappa)\delta(p'_a - p_a)\delta(p'_b - p_b) = \delta(P' + \kappa' n - P - \kappa n)\delta(p'_a - p_a)\delta(p'_b - p_b)\,, \tag{4.7}$$

showing the overall 4-momentum conservation for the R-matrix, including the momentum spurions. The M-amplitudes satisfy the Kadyshevsky equation

$$\begin{aligned} M_{\kappa',\kappa}(p'_a, p'_b; p_a, p_b) \ &= \ I_{\kappa',\kappa}(p'_a, p'_b; p_a, p_b) + \int d^4p''_a \int d^4p''_b \int d\kappa'' I_{\kappa'\kappa''}(p'_a, p'_b; p''_a, p''_b)\cdot \\ &\quad \times G_{\kappa''}(p''_a, p''_b) M_{\kappa'',\kappa}(p''_a, p''_b; p_a, p_b)\cdot \delta(p''_a + p''_b + \kappa'' n - p_a - p_b - \kappa n), \end{aligned} \tag{4.8}$$

which is displayed in Fig. 1. Here the propagation of the two nucleons and of the quasi-particle is described by

$$G_\kappa(p_a, p_b)_{\alpha',\beta';\alpha,\beta} \ = \ \frac{-1}{(2\pi)^2}\delta(p_a^2 - M_a^2)\delta(p_b^2 - M_b^2)\cdot G_0(\kappa)\,. \tag{4.9}$$

V. THREE-DIMENSIONAL TWO-BODY EQUATIONS

The Kadyshevsky analog (4.8) of the Bethe-Salpeter equation we write in the form

$$\begin{aligned} &M_{\kappa',\kappa}(p'_a, p'_b; p_a, p_b) = I_{\kappa',\kappa}(p'_a, p'_b; p_a, p_b) + \int d^4p''_a \int d^4p''_b \int d\kappa''\cdot \\ &\times I_{\kappa',\kappa''}(p'_a, p'_b; p''_a, p''_b) G_{\kappa''}(p''_a, p''_b) M_{\kappa'',\kappa}(p''_a, p''_b; p_a, p_b)\cdot \\ &\times \delta(p''_a + p''_b + \kappa'' n - p_a - p_b - \kappa n)\,. \end{aligned} \tag{5.1}$$

[1] For a general field-theoretical treatment of the Kadyshevsky approach to relativistic two-body scattering, see Refs. [33, 34].

In the CM-frame we have

$$P = (W, \mathbf{0}) \ , \ \ p = (0, \mathbf{p}) \ ; P' = (W', \mathbf{0}) \ , \ \ p' = (0, \mathbf{p}') \, . \tag{5.2}$$

Following [15, 17] we assume that the unit vector n^μ, which defines the time axis, is collinear to $P = p_a + p_b$ and hence also to $P' = p'_a + p'_b$. Then [2]

$$n^\mu = \frac{p_a^\mu + p_b^\mu}{\sqrt{(p_a + p_b)^2}} = \frac{p_a'^\mu + p_b'^\mu}{\sqrt{(p'_a + p'_b)^2}} \xrightarrow{CM} (1, \mathbf{0}) \, . \tag{5.3}$$

In the CM-variables, equation (5.1), for the $(+,+)$-components only, reads

$$\begin{aligned} &M_{\kappa',\kappa}(p', W'; p, W) = I_{\kappa',\kappa}(p', W'; p, W) + \int dW'' \int d^4p'' \int d\kappa'' \cdot \\ &\times I_{\kappa',\kappa''}(p', W'; p'', W'') G_{\kappa''}(p'', W'') M_{\kappa''}(p'', W''; p, W) \cdot \\ &\times \delta\left[W'' - W + (\kappa'' - \kappa) n_0\right] \, . \end{aligned} \tag{5.4}$$

In the CM-frame, the two-nucleon propagator (4.9) becomes

$$G_\kappa(W'', p'') \ = \ \frac{-1}{(2\pi)^2} \delta\left(\frac{1}{2}W'' + p_0'' - E_a''\right) \delta\left(\frac{1}{2}W'' - p_0'' - E_b''\right) G_0(\kappa'') \, . \tag{5.5}$$

Now, the integrations over W'', p_0'', and κ'' can be carried through in (5.4) giving

$$\begin{aligned} &M_{\kappa',\kappa}(\mathbf{p}', W'; \mathbf{p}, W) = I_{\kappa',\kappa}(\mathbf{p}', W'; \mathbf{p}, W) + \int \frac{d^3p''}{(2\pi)^3} \cdot \\ &\times I_{\kappa',\kappa''}(\mathbf{p}', W'; \mathbf{p}'', W'') \left(\frac{M_a M_b}{E_a'' E_b''}\right) \frac{1}{\sqrt{s''} - \left(\sqrt{s} + \kappa\right) - i\epsilon} M_{\kappa'',\kappa}(\mathbf{p}'', W''; \mathbf{p}, W) \, , \end{aligned} \tag{5.6}$$

with the constraints

$$W \ = \ \sqrt{s} \ , \ \ W' = \sqrt{s'} = \sqrt{s} + \kappa - \kappa' \ , \ W'' = \sqrt{s''} = E_a'' + E_b'' \, . \tag{5.7}$$

We notice that the left-half-off-shell M-matrix satisfies an integral equation of the type

$$M_{\kappa',0} = I_{\kappa',0} + \int \ I_{\kappa',\kappa''} \ G_{\kappa''} \ M_{\kappa'',0}$$

where the κ's are all fixed in terms of the momenta of the particles, since

$$\kappa' = \sqrt{s} - \sqrt{s'} \ \ , \ \ \kappa'' = \sqrt{s} - \sqrt{s''} \, .$$

Defining the T-matrix etc. in terms of the left-half-off-shell M-matrix , and the quasi-potential K in terms of the both left and right off-shell interaction kernel I, by

$$T(\mathbf{p}', \mathbf{p}; W) \ = \ M_{\kappa',\kappa=0}(\mathbf{p}', W'; \mathbf{p}, W) \, , \ K(\mathbf{p}', \mathbf{p}; W) = I_{\kappa',\kappa=0}(\mathbf{p}', W'; \mathbf{p}, W) \, , \tag{5.8}$$

we will have, instead of (5.6),

$$T(\mathbf{p}', \mathbf{p}; W) \ = \ K(\mathbf{p}', \mathbf{p}; W) + \int \frac{d^3p''}{(2\pi)^3} K(\mathbf{p}', \mathbf{p}''; W) \left(\frac{M_a M_b}{E_a'' E_b''}\right) \frac{1}{\sqrt{s''} - \sqrt{s}} T(\mathbf{p}'', \mathbf{p}; W), \tag{5.9}$$

[2] Notice that with this choice for n^μ, the four-velocity of the system is conserved even off the energy-shell.

which is the so-called 'quasi-potential' equation. The quantity K playing the role of a potential is in general a complicated function of the energy W and is called a 'quasi-potential'. Notice, that for $\varkappa = 0$, one has $\varkappa' = \sqrt{s} - \sqrt{s'}$, and so $\varkappa'$ is fixed by $p = |\mathbf{p}|$ and $p' = |\mathbf{p}'|$.

For equal masses, i.e. $M_a = M_b = M$, we have

$$E''_a \;=\; E''_b = E(\mathbf{p}'')\,, s = 4E^2(\mathbf{p}) = 4(p^2 + M^2)\,, s'' = 4E^2(\mathbf{p}'') = 4(p''^2 + M^2). \tag{5.10}$$

Then, (5.9) goes over into the equation

$$T(\mathbf{p}', \mathbf{p}; W) \;=\; K(\mathbf{p}', \mathbf{p}; W) + \frac{1}{(2\pi)^3} \int \frac{d^3p''}{2E(\mathbf{p}'')}\, K(\mathbf{p}', \mathbf{p}''; W)\, \frac{M^2}{E(\mathbf{p}'')\,]E(\mathbf{p}'') - E(\mathbf{p}) - i\epsilon]}\, T(\mathbf{p}'', \mathbf{p}; W) \tag{5.11}$$

which is the quasi-potential equation of Kadyshevsky, see [16] equation (3.33).

In Appendix A the Bethe-Goldstone-Kadyshevsky equation and the corresponding "relativistic" G-matrix are given.

VI. LIPPMANN-SCHWINGER AND BETHE-GOLDSTONE EQUATION

The Lippmann-Schwinger amplitude is obtained from (5.11) by the transformation

$$\mathcal{T}(\mathbf{p}', \mathbf{p}) = N(\mathbf{p}')\, T(\mathbf{p}', \mathbf{p})\, N(\mathbf{p})\,,\;\; \mathcal{V}(\mathbf{p}', \mathbf{p}) = N(\mathbf{p}')\, K(\mathbf{p}', \mathbf{p})\, N(\mathbf{p}), \tag{6.1}$$

with $N(\mathbf{p}) = M/(\sqrt{2}E(\mathbf{p}))$. Then, the non-relativistic Lippmann-Schwinger equation is obtained by using in the Green-function and the potential the non-relativistic approximation $E(\mathbf{p}) \approx M + \mathbf{p}^2/2M$ giving

$$\mathcal{T}(\mathbf{p}', \mathbf{p}) \;=\; \mathcal{V}(\mathbf{p}', \mathbf{p}) + \frac{1}{(2\pi)^3} \int \frac{d^3p''}{2E(\mathbf{p}'')}\, \mathcal{V}(\mathbf{p}', \mathbf{p}'')\, \frac{M}{(\mathbf{p}''^2 - \mathbf{p}^2 - i\epsilon)}\, \mathcal{T}(\mathbf{p}'', \mathbf{p}). \tag{6.2}$$

For the details of the formalism of spin 1/2-1/2 scattering, using the expansion in Pauli-invariants, we refer to the papers of the ESC-model e.g. [35, 36].

The corresponding Bethe-Goldstone equation reads

$$\begin{aligned} G(\mathbf{p}', \mathbf{p}) \;=\; & V(\mathbf{p}', \mathbf{p}) + \int \frac{d^3p''}{(2\pi)^3}\, V(\mathbf{p}', \mathbf{p}'') \cdot \\ & \times Q_P(\mathbf{p}''; p_F)\, g(\mathbf{p}''; W)\, G(\mathbf{p}'', \mathbf{p}) \end{aligned} \tag{6.3}$$

with the standard Green function and Pauli projection operator

$$g(\mathbf{p}; W) = \frac{M_n}{\mathbf{p}_i^2 - \mathbf{p}^2 + i\delta},\; Q_P(\mathbf{p}''; p_F) = 1 - n_F(\mathbf{p}''). \tag{6.4}$$

The corrections to the approximation $E_2^{(+)} \approx g(\mathbf{p}; W)$ are of order $1/M^2$, which we neglect henceforth.

The transition from Dirac-spinors to Pauli-spinors, is given in Appendix C of Ref. [37], where we write for the the Bethe-Goldstone equation in the 4-dimensional Pauli-spinor space

$$\begin{aligned} \mathcal{G}(\mathbf{p}', \mathbf{p}) \;=\; & \mathcal{V}(\mathbf{p}', \mathbf{p}) + \int \frac{d^3p''}{(2\pi)^3}\, \mathcal{V}(\mathbf{p}', \mathbf{p}'') \cdot \\ & \times Q_P(\mathbf{p}''; p_F)\, g(\mathbf{p}''; W)\, \mathcal{G}(\mathbf{p}'', \mathbf{p})\,. \end{aligned} \tag{6.5}$$

The $\mathcal{G}$-operator in Pauli spinor-space is defined by

$$\chi^{(a)\dagger}_{\sigma'_a}\chi^{(b)\dagger}_{\sigma'_b}\ \mathcal{G}(\mathbf{p}',\mathbf{p})\ \chi^{(a)}_{\sigma_a}\chi^{(b)}_{\sigma_b} = \\ \bar{u}_a(\mathbf{p}',\sigma'_a)\bar{u}_b(-\mathbf{p}',\sigma'_b)\ \tilde{G}(\mathbf{p}',\mathbf{p})\ u_a(\mathbf{p},\sigma_a)u_b(-\mathbf{p},\sigma_b). \tag{6.6}$$

and similarly for the $\mathcal{V}$-operator. Like in the derivation of the OBE-potentials [38–40] we make the off-shell and on-shell the approximation, $E(\mathbf{p}) = M + \mathbf{p}^2/2M$ and $W = 2\sqrt{\mathbf{p}_i^2 + M^2} = 2M + \mathbf{p}_i^2/M$, everywhere in the interaction kernels, which, of course, is fully justified for low energies only. In contrast to these kinds of approximations, of course the full $\mathbf{k}^2$-dependence of the form factors is kept throughout the derivation of the TME. Notice that the gaussian form factors suppress the high momentum transfers strongly. This means that the contribution to the potentials from intermediate states which are far off-energy-shell can not be very large.

Because of rotational invariance and parity conservation, the $\mathcal{G}$-matrix, which is a 4×4-matrix in Pauli-spinor space, can be expanded into the following set of in general 8 spinor invariants, see for example Ref. [41]. Introducing [42]

$$\mathbf{q} = \frac{1}{2}(\mathbf{p}' + \mathbf{p})\ ,\ \mathbf{k} = \mathbf{p}' - \mathbf{p}\ ,\ \mathbf{n} = \mathbf{p}\times\mathbf{p}', \tag{6.7}$$

with, of course, $\mathbf{n} = \mathbf{q}\times\mathbf{k}$, we choose for the operators P_j in spin-space

$$\begin{aligned} P_1 &= 1, \quad P_2 = \boldsymbol{\sigma}_1\cdot\boldsymbol{\sigma}_2, \\ P_3 &= (\boldsymbol{\sigma}_1\cdot\mathbf{k})(\boldsymbol{\sigma}_2\cdot\mathbf{k}) - \frac{1}{3}(\boldsymbol{\sigma}_1\cdot\boldsymbol{\sigma}_2)\mathbf{k}^2, \\ P_4 &= \frac{i}{2}(\boldsymbol{\sigma}_1+\boldsymbol{\sigma}_2)\cdot\mathbf{n}, \quad P_5 = (\boldsymbol{\sigma}_1\cdot\mathbf{n})(\boldsymbol{\sigma}_2\cdot\mathbf{n}), \\ P_6 &= \frac{i}{2}(\boldsymbol{\sigma}_1-\boldsymbol{\sigma}_2)\cdot\mathbf{n}, \\ P_7 &= (\boldsymbol{\sigma}_1\cdot\mathbf{q})(\boldsymbol{\sigma}_2\cdot\mathbf{k}) + (\boldsymbol{\sigma}_1\cdot\mathbf{k})(\boldsymbol{\sigma}_2\cdot\mathbf{q}), \\ P_8 &= (\boldsymbol{\sigma}_1\cdot\mathbf{q})(\boldsymbol{\sigma}_2\cdot\mathbf{k}) - (\boldsymbol{\sigma}_1\cdot\mathbf{k})(\boldsymbol{\sigma}_2\cdot\mathbf{q}). \end{aligned} \tag{6.8}$$

Here we follow Ref. [40], where in contrast to Ref. [39], we have chosen P_3 to be a purely 'tensor-force' operator. The expansion in spinor-invariants reads

$$\mathcal{G}(\mathbf{p}',\mathbf{p}) = \sum_{j=1}^{8}\ \widetilde{G}_j(\mathbf{p}'^2,\mathbf{p}^2,\mathbf{p}'\cdot\mathbf{p})\ P_j(\mathbf{p}',\mathbf{p})\ . \tag{6.9}$$

Similarly to (6.9) we expand the potentials V. In the case of the axial-vector meson exchange there will occur terms proportional to

$$P'_5 = (\boldsymbol{\sigma}_1\cdot\mathbf{q})(\boldsymbol{\sigma}_2\cdot\mathbf{q}) - \frac{1}{3}(\boldsymbol{\sigma}_1\cdot\boldsymbol{\sigma}_2)\mathbf{q}^2. \tag{6.10}$$

The proper treatment of such a (non-local) Pauli-invariant has been developed for the ESC16-models, which is described in [9], Appendix B . For the treatment of the potentials with P_8 we use the identity [43]

$$P_8 = -(1+\boldsymbol{\sigma}_1\cdot\boldsymbol{\sigma}_2)P_6. \tag{6.11}$$

Under time-reversal $P_7 \to -P_7$ and $P_8 \to -P_8$. Therefore for elastic scattering $V_7 = V_8 = 0$. Anticipating the explicit results for the potentials in section IV A we notice the following: (i) For the general

BB-reaction we will find no contribution to V_7. The operators P_6 and P_8 give spin singlet-triplet transitions. (ii) In the case of non-strangeness-exchange ($\Delta S = 0$), $V_6 \neq 0$ and V_8=0. The latter follows from our approximation to neglect the mass differences among the nucleons, between the Λ and Σ's, and among the Ξ's. (iii) In the case of strangeness-exchange ($\Delta S = \pm 1$), $V_6, V_8 \neq 0$. The contributions to V_6 come from graphs with both spin- and particle-exchange, i.e. Majorana-type potentials having the $P_f P_\sigma P_6 = -P_x P_6$-operator. Here, $P_f P_\sigma$ reflect our convention for the two-particle wave functions, see [38]. The contributions to V_8 come from graphs with particle-exchange and spin-exchange, because $P_8 = -P_\sigma P_6$. Therefore, we only have to apply P_f in order to map the wave functions after such exchange onto our two-particle wave-functions. So, we have the $P_f P_8 = +P_x P_6$-operator. Here, we used that for BB-systems the allowed physical states satisfy $P_f P_\sigma P_x = -1$.
In the SU(6) quark model [3], instead of the Pauli-spinors, one uses for the quarks the Dirac-spinors

$$u_i^{(0)}(\mathbf{p}_i) = \sqrt{\frac{E_i + m_i}{2m_i}} \begin{bmatrix} 1 \\ \frac{\sigma_i \cdot \mathbf{p}_i}{E_i + m_i} \end{bmatrix} \otimes \chi_i, \tag{6.12}$$

where $\mathbf{p}_{\mathbf{i}_i}$ denotes the three-momentum of the quarks in e.g. the CM-system.

VII. EXTENDED-SOFT-CORE QQM AND NNM INTERACTIONS

In the ESC-model there are single- and pair-meson quark-quark couplings. They are the basis for the OBE, TME and MPE potentials. The nucleon-nucleon-meson (NNM) interactions have been described in detail in [9]. Therefore, we restrict ourselves in this section to the quark-quark-meson (QQM) interactions. The meson-quark couplings are designed such as to reproduce the ESC-potentials for baryon-baryon when folded in with the constituent quark wave functions of the SU(6) quark-model. Strictly, for the TME and MPE potentials a modification should be made in the presence of quark matter. In this paper such quark density corrections are omitted.

A. Meson-quark-quark Interactions

The potential of the ESC-model contains the contributions from (i) One-boson-exchanges, (ii) Uncorrelated Two-Pseudo-scalar exchange, and (iii) Meson-Pair-exchange. In this section we review the potentials and indicate the changes with respect to earlier papers on the OBE- and ESC-models. The spin-1 meson-exchange is an important ingredient for the baryon-baryon force. In the ESC16-model we treat the vector-mesons and the axial-vector mesons according to the Proca- [44] and the B-field- [45, 46] formalism respectively. For details, we refer to [9], Appendix C.

B. One-Boson-Exchange Interactions in Momentum Space

The local interaction Hamilton densities for the different couplings are [47]

a) Pseudoscalar-meson exchange ($J^{PC} = 0^{-+}$)

$$\mathcal{H}_{pv}(x) = \frac{f_{pv}}{m_{\pi^+}} \bar{q}(x) \gamma_\mu \gamma_5 q(x) \partial^\mu \phi_P(x). \tag{7.1}$$

This is the pseudovector coupling, and the relation with the pseudoscalar coupling is $g_p = 2m_Q/m_{\pi^+}$, where m_Q is the quark mass.

b) Vector-meson exchange ($J^{PC} = 1^{--}$)

$$\begin{aligned}\mathcal{H}_v^{1)} &= g_v \bar{q}(x)\gamma_\mu q(x)\phi_V^\mu + \frac{f_v}{4\mathcal{M}}\bar{q}(x)\sigma_{\mu\nu}q(x)(\partial^\mu\phi_V^\nu - \partial^\nu\phi_V^\mu) \\ &= \left[(\bar{q}(x)\gamma_\mu q(x))\, f_{1,v} + \frac{i}{2}\left(\bar{q}(x)\overset{\leftrightarrow}{\partial}_\mu q(x)\right) f_{2,v}\right]\cdot\phi_V^\mu,\end{aligned} \tag{7.2}$$

where $\sigma_{\mu\nu} = i[\gamma_\mu, \gamma_\nu]/2$, and $f_{1,v} = g_v + (m_Q/\mathcal{M})f_v$, $f_{2,v} = -f_v/\mathcal{M}$. The scaling mass $\mathcal{M}$ will be taken to be the proton mass. The Gordon decomposition

$$\partial_\nu\,[\bar{q}(x)\sigma^{\mu\nu}q(x)] = 2\bar{m}_Q\bar{q}(x)\gamma^\mu q(x) + i\bar{q}(x)\overset{\leftrightarrow}{\partial}{}^\mu q(x)$$

with $\bar{m}_Q = \left(m'_Q + m_Q\right)$, shows that the magnetic-coupling consists of a pure vector and scalar bilinear quark-field part. As deduced in [1], an extra interaction is needed in order to give the correct structure of the baryon-baryon potential. Therefore, on the quark-level we add the interaction

$$\mathcal{H}_v^{2)} = -\frac{\Box}{4m_Q^2}\left[[\bar{q}(x)\gamma_\mu q(x)]f'_{1,v} + \left(i\bar{q}(x)\overset{\leftrightarrow}{\partial}_\mu q(x)\right)f'_{2,v}\right]\cdot\phi_V^\mu,$$

where $f'_{1,v} = (4/9)f_{1,v}$, $f'_{2,v} = (4/9)f_{2,v}$. Then, the total vector-exchange interaction is

$$\begin{aligned}\mathcal{H}_v &= \bar{g}_v\bar{q}(x)\gamma_\mu q(x)\phi_V^\mu + \frac{\bar{f}_v}{4\mathcal{M}}\bar{q}(x)\sigma_{\mu\nu}q(x)(\partial^\mu\phi_V^\nu - \partial^\nu\phi_V^\mu), \\ \bar{g}_v &= g_v\left(1 - \frac{g'_v}{g_v}\frac{\Box}{4m_Q^2}\right),\ \bar{f}_v = f_v\left(1 - \frac{f'_v}{f_v}\frac{\Box}{4m_Q^2}\right).\end{aligned} \tag{7.3}$$

An attractive alternative to the inclusion of the (g'_v, f'_v)-couplings would be to have a zero in the QQV form factors. For $g'_v/g_v = f'_v/f_v = 4/9$ this zero is at $\mathbf{k}^2 = M_N^2$, *i.e.* a short range effect.

c) Axial-vector-meson exchange ($J^{PC} = 1^{++}$, 1^{st} kind):

$$\mathcal{H}_a^{(1)} = g_a[\bar{q}(x)\gamma_\mu\gamma_5 q(x)]\phi_A^\mu + \frac{if_a}{\mathcal{M}}[\bar{q}(x)\gamma_5 q(x)]\,\partial_\mu\phi_A^\mu. \tag{7.4}$$

We impose axial-current conservation by the relation $f_a = \left(m_{A_1}^2/(2m_Q\mathcal{M}\right)^{-1} g_a$ [48]. The details of the treatment of the axial-vector mesons are given in [9], Appendix B. It was found in [1] that the correct reproduction of the baryon-baryon spin-orbit potential obtained by a folding of the axial-exchange between quarks requires the additional interaction

$$\mathcal{H}_a^{(2)} = -i\frac{g'_a}{\mathcal{M}^2}\{\varepsilon_{\mu\nu\alpha\beta}[\partial^\alpha\bar{q}(x)\gamma^\nu\partial^\beta q(x)]\}\cdot\phi_A^\mu \tag{7.5}$$

with $g'_a = g_a$.

d) Axial-vector-meson exchange ($J^{PC} = 1^{+-}$, 2^{nd} kind):

$$\mathcal{H}_b = \frac{if_b}{m_B}[\bar{q}(x)\sigma_{\mu\nu}\gamma_5 q(x)\,\partial^\nu\phi_B^\mu\,. \tag{7.6}$$

Like for the axial-vector mesons of the 1^{st}-kind we include an SU(3)-nonet with members $b_1(1235), h_1(1170), h_1(1380)$. In the quark-model they are $Q\bar{Q}(^1P_1)$-states.

e) Scalar-meson exchange ($J^{PC} = 0^{++}$):

$$\mathcal{H}_s = g_s \left\{ g_s - \frac{g_s'}{g_s} \frac{\Box}{4m_Q^2} \right\} [\bar{q}(x)q(x)] \cdot \phi_S, \tag{7.7}$$

with $g_s'/g_s = -8/9$. Again, the requirement from the folding of meson-exchange between quarks into the baryon gives $g_s' \approx -g_s$. It is clear that inclusion of the g_s' does not introduce a zero in the scalar-quark-quark coupling. The additional contribution from the g_s' coupling is taken onto account easily. In the ESC-models we include a zero in the form factor, which we also keep in the quark-quark potential.
f) Pomeron-exchange ($J^{PC} = 0^{++}$): The vertices for this 'diffractive'-exchange have the same Lorentz structure as those for scalar-meson-exchange.

g) Odderon-exchange ($J^{PC} = 1^{--}$):

$$\mathcal{H}_O = g_O[\bar{\psi}\gamma_\mu\psi]\phi_O^\mu + \frac{f_O}{4\mathcal{M}}[\bar{\psi}\sigma_{\mu\nu}\psi](\partial^\mu\phi_O^\nu - \partial^\nu\phi_O^\mu). \tag{7.8}$$

Since the gluons are flavorless, Odderon-exchange is treated as an SU(3)-singlet. Furthermore, since the Odderon represents a Regge-trajectory with an intercept equal to that of the Pomeron, and is supposed not to contribute for small $\mathbf{k}^2$, we include a factor $\mathbf{k}^2/\mathcal{M}^2$ in the coupling.

Including form factors $f(\mathbf{x}' - \mathbf{x})$, the interaction hamiltonian densities are modified to

$$H_X(\mathbf{x}) = \int d^3x'\, f(\mathbf{x}' - \mathbf{x})\mathcal{H}_X(\mathbf{x}'), \tag{7.9}$$

for $X = P,\ V,\ A$, and S (P = pseudo-scalar, V = vector, A = axial-vector, and S = scalar). The potentials in momentum space are the same as for point interactions, except that the coupling constants are multiplied by the Fourier transform of the form factors.

In the derivation of the V_i we employ the same approximations as in [39, 40], i.e.

1. We expand in $1/M$: $E(p) = \left[\mathbf{k}^2/4 + \mathbf{q}^2 + M^2\right]^{\frac{1}{2}}$
   $\approx M + \mathbf{k}^2/8M + \mathbf{q}^2/2M$ and keep only terms up to first order in $\mathbf{k}^2/M$ and $\mathbf{q}^2/M$. This except for the form factors where the full $\mathbf{k}^2$-dependence is kept throughout the calculations. Notice that the gaussian form factors suppress the high $\mathbf{k}^2$-contributions strongly.

2. In the meson propagators $(-(p_1 - p_3)^2 + m^2) \approx (\mathbf{k}^2 + m^2)$.

3. When two different baryons are involved at a BBM-vertex their average mass is used in the potentials and the non-zero component of the momentum transfer is accounted for by using an effective mass in the meson propagator (for details see [40]).

Due to the approximations we get only a linear dependence on $\mathbf{q}^2$ for V_1. In the following, separating the local and the non-local parts, we write

$$V_i(\mathbf{k}^2, \mathbf{q}^2) = V_{ia}(\mathbf{k}^2) + V_{ib}(\mathbf{k}^2)(\mathbf{q}^2 + \frac{1}{4}\mathbf{k}^2), \tag{7.10}$$

where in principle $i = 1, 8$.

The OBE-potentials are now obtained in the standard way (see e.g. [39, 40]) by evaluating the BB-interaction in Born-approximation. We write the potentials V_i of Eqs. (7.10) in the form

$$V_i(\mathbf{k}^2, \mathbf{q}^2) = \sum_X \Omega_i^{(X)}(\mathbf{k}^2) \cdot \Delta^{(X)}(\mathbf{k}^2, m^2, \Lambda^2). \tag{7.11}$$

Furthermore for $X = P, V$

$$\Delta^{(X)}(\mathbf{k}^2, m^2, \Lambda^2) = e^{-\mathbf{k}^2/\Lambda^2} / \left(\mathbf{k}^2 + m^2\right), \tag{7.12}$$

and for $X = S, A$ a zero in the form factor

$$\Delta^{(S)}(\mathbf{k}^2, m^2, \Lambda^2) = \left(1 - \mathbf{k}^2/U^2\right)\, e^{-\mathbf{k}^2/\Lambda^2} / \left(\mathbf{k}^2 + m^2\right), \tag{7.13}$$

and for $X = D, O$

$$\Delta^{(D)}(\mathbf{k}^2, m^2, \Lambda^2) = \frac{1}{\mathcal{M}^2} e^{-\mathbf{k}^2/(4m_{P,O}^2)}. \tag{7.14}$$

In the latter expression $\mathcal{M}$ is a universal scaling mass, which is again taken to be the proton mass. The mass parameter m_P controls the $\mathbf{k}^2$-dependence of the Pomeron-, f-, f'-, A_2-, and $K^{\star\star}$-potentials. Similarly, m_O controls the $\mathbf{k}^2$-dependence of the Odderon.

In the following we give the OBE-potentials in momentum-space for the hyperon-nucleon systems. From these those for NN and YY can be deduced easily. We assign the particles 1 and 3 to be hyperons, and particles 2 and 4 to be nucleons. Mass differences among the hyperons and among the nucleons will be neglected.

C. The Meson-Pair Interactions

For the phenomenological SU(2) meson-pair interactions the Hamiltonians, for meson-pairs with quantum numbers (J,P,C), for the non-strange quarks i.e. below $q(x) \equiv Q_1(x)$, are

$$\begin{aligned}
J^{PC} = 0^{++} :\ \mathcal{H}_S &= \bar{q}(x)q(x)\ \left[g_{(\pi\pi)_0}\boldsymbol{\pi}\cdot\boldsymbol{\pi} + g_{(\sigma\sigma)}\sigma^2\right]/m_\pi, && (7.15a)\\
\mathcal{H}_E &= \bar{q}(x)\boldsymbol{\tau}q(x)\cdot\boldsymbol{\pi}\left[g_{(\pi\eta)}\eta + g_{(\pi\eta')}\eta'\right]/m_\pi, && (7.15b)\\
\mathcal{H}_{S_2} &= \bar{q}(x)q(x)\, h_{(\pi\pi)_0}\partial_\mu\boldsymbol{\pi}\cdot\partial^\mu\boldsymbol{\pi}/m_\pi^3, && (7.15c)\\
J^{PC} = 1^{--} :\ \mathcal{H}_V &= g_{(\pi\pi)_1}\bar{q}(x)\gamma_\mu\boldsymbol{\tau}q(x)\cdot(\boldsymbol{\pi}\times\partial^\mu\boldsymbol{\pi})/m_\pi^2 \\
&\quad -\frac{f_{(\pi\pi)_1}}{2\mathcal{M}}\bar{q}(x)\sigma_{\mu\nu}\boldsymbol{\tau}q(x)\partial^\nu\cdot(\boldsymbol{\pi}\times\partial^\mu\boldsymbol{\pi})/m_\pi^2, && (7.15d)\\
J^{PC} = 1^{++} :\ \mathcal{H}_A &= g_{(\pi\rho)_1}\bar{q}(x)\gamma_5\gamma_\mu\boldsymbol{\tau}q(x)\cdot(\boldsymbol{\pi}\times\boldsymbol{\rho}^\mu)/m_\pi, && (7.15e)\\
\mathcal{H}_P &= g_{(\pi\sigma)}\bar{q}(x)\gamma_5\gamma_\mu\boldsymbol{\tau}q(x)\cdot(\boldsymbol{\pi}\partial^\mu\sigma - \sigma\partial^\mu\boldsymbol{\pi})/m_\pi^2 \\
&\quad + g_{(\pi P)}\bar{q}(x)\gamma_5\gamma_\mu\boldsymbol{\tau}q(x)\cdot(\boldsymbol{\pi}\partial^\mu P - P\partial^\mu\boldsymbol{\pi})/m_\pi^2, && (7.15f)\\
J^{PC} = 1^{+-} :\ \mathcal{H}_H &= -ig_{(\pi\rho)_0}\bar{q}(x)\gamma_5\sigma_{\mu\nu}q(x)\partial^\nu(\boldsymbol{\pi}\cdot\boldsymbol{\rho}^\mu)/m_\pi^2, && (7.15g)\\
\mathcal{H}_B &= -ig_{(\pi\omega)}\bar{q}(x)\gamma_5\sigma_{\mu\nu}\boldsymbol{\tau}q(x)\cdot\partial^\nu(\boldsymbol{\pi}\,\omega^\mu)/m_\pi^2. && (7.15h)
\end{aligned}$$

For the SU(3) generalization see Ref. [36] section III.

In Eq. (7.15) also the Pomeron contribution is listed, but in recent ESC-models $g_{(\pi P)} = 0$. The same is true for the $\mathcal{H}_{S_2}$ interaction, which we will discuss in connection with the FM three-body force [49, 50].

As for the scaling of the pair-coupling parameters, the π^+-mass was choosen. For the operators $\partial^\mu\pi(x)$ this follows the non-linear chiral models. The other scaling m_π-factors may be could be better replaced by M, the nucleon mass. This would presumably represent better the scale of the physics involved. For example pair-couplings from $N\bar{N}$-pairs ('negative-energy states') would be parameterized more naturally this way. However, in our works on the ESC-model we sofar always used the m_π-mass as a scaling parameter, and therefore we will do this also in this paper.

VIII. CHANNELS, POTENTIALS, AND $SU(3)$ SYMMETRY

A. Channels and Potentials

In this paper we consider the quark-quark and quark-nucleon reactions with strangeness S=0:

$$Q(s_a, i_a) + Q(s_b, i_b) \;\rightarrow\; Q(s'_a, i'_a) + Q(s'_b, i'_b), \tag{8.1a}$$
$$Q(s_a, i_a) + N(s_b, i_b) \;\rightarrow\; Q(s'_a, i'_a) + N(s'_b, i'_b), \tag{8.1b}$$

where $Q = U, D$ and $N = P, N$ are iso-doublets. The 3-components of the spins and isospins are $\pm 1/2$. Like in Ref.'s [40] we will also refer to a and a' as particles 1 and 3, and to b and b' as particles 2 and 4. For the kinematics and the definition of the amplitudes, we refer to papers [35, 36] of the series of papers on the ESC04 model. Here we note that both the BB- and QQ-channels are of the same type, nanely spin-1/2-spin 1/2 scattering. Similar material can be found in [40]. Also, in paper I the derivation of the Lippmann-Schwinger equation in the context of the relativistic two-body equation is described.

For the quark-quark and quark-nucleon there are three channels with different charges for the baryon-number B:

$$B = 2/3 : \begin{cases} q = +4/3 : & UU \rightarrow UU, \\ q = +1/3 : & UD \rightarrow UD, \\ q = -2/3 : & DD \rightarrow DD, \end{cases} \tag{8.2a}$$

$$B = 4/3 : \begin{cases} q = +5/3 : & UP \rightarrow UP, \\ q = +2/3 : & UN \rightarrow UN, \\ q = +2/3 : & DP \rightarrow DP, \\ q = -1/3 : & DN \rightarrow DN, \end{cases} \tag{8.2b}$$

(8.2c)

Note that since the spin and isospin of these quarks and the nucleons are identical the spin and isospin factors of the potentials are completely analogous to that for the nucleon-nucleon potentials. Therefore, we refer for these factors to the NN-papers, e.g. [35] etc..

Like in [35, 40], the potentials are calculated on the isospin basis. there are only two isospin channels: (i) $I = 1 :\ (UU, (UD+DU)/\sqrt{2}, DD)$, and (ii) $I = 0 :\ (UD-DU)/\sqrt{2}$. Similarly for the QN-channels.

In this work we give the QQ- and the QN-potentials for the Lippmann-Schwinger equation in momentum space, and the Schrödinger equation in configuration space.

The momentum space and configuration space potentials for the ESC models have been described in papers [35] and [9] for baryon-baryon in general. Also in the ESC-model, the potentials are of such a form that they are exactly equivalent in both momentum space and configuration space. The treatment of the mass differences among the quarks are handled exactly similar as is done in [40]. Also, exchange potentials related to strange meson exchange K, K^* etc. , can be found in these references.

The quark mass differences in the intermediate states for TME- and MPE- potentials will be neglected for QQ-scattering. This, although possible in principle, becomes rather laborious and is not expected to change the characteristics of the quark-quark potentials much.

B. QQM-couplings in $SU(3)$, Matrix-representation

The $Q = (U, D, S)$-quarks are in the fundamental {3}-irrep, and in matrix notation represented by a collumn. In previous work of the Nijmegen group, e.g. [40], the treatment of $SU(3)$ has been given in detail for the BBM interaction Lagrangians and the coupling coefficients of the OBE-graphs. However, for the ESC-models we also need the coupling coefficients for the TME- and the MPE-graphs. Since there are many more TME- and MPE-graphs than OBE-graphs, an computerized computation is desirable. As in the baryon-baryon papers, here the so-called 'cartesian-octet'-representation for the mesons is quite useful. Therefore, we give an exposition of this representation, its connection with the matrix representation used in our previous work, and the formulation of the coupling coefficients used in the automatic computation.

The various meson nonets (we take the pseudoscalar mesons with $J^P = 0^+$ as an example), see e.g. [51, 52], are represented by

$$P = P_{\{1\}} + P_{\{8\}}, \tag{8.3}$$

where the singlet matrix $P_{\{1\}}$ has elements $\eta_0/\sqrt{3}$ on the diagonal, and the octet matrix $P_{\{8\}}$ is given by

$$P_{\{8\}} = \begin{pmatrix} \frac{\pi^0}{\sqrt{2}} + \frac{\eta_8}{\sqrt{6}} & \pi^+ & K^+ \\ \pi^- & -\frac{\pi^0}{\sqrt{2}} + \frac{\eta_8}{\sqrt{6}} & K^0 \\ K^- & \overline{K^0} & -\frac{2\eta_8}{\sqrt{6}} \end{pmatrix}. \tag{8.4}$$

The $SU(3)$-invariant BBP-interaction Lagrangian can be written as [51]

$$\mathcal{H}_I \;=\; g_8 \sum_{p=1}^{8} \left[\bar{Q}_a \left(\lambda_p\right)_{ab} Q_b\right] \phi_{8,p} + g_1 \; \left[\bar{Q}Q\right] \; \phi_9. \tag{8.5}$$

where g_8 and g_1 are the singlet and octet couplings. We write the octet coupling in the form of the meson matrix M:

$$\mathcal{H}_I(8) = g_8\sqrt{2}\left[\bar{Q}M^{(8)}Q_b\right], \;\; M^{(8)}_{ab} = \sum_{p=1}^{8} \left(\lambda_p\right)_{ab} \phi_{8,p}. \tag{8.6}$$

The convention used for the isospin doublets is

$$n = \begin{pmatrix} u \\ d \end{pmatrix}, \; K = \begin{pmatrix} K^+ \\ K^0 \end{pmatrix}, \; K_c = \begin{pmatrix} \overline{K^0} \\ -K^- \end{pmatrix}. \tag{8.7}$$

Working out (8.5) on the isospin basis we have

$$\begin{aligned}\mathcal{H}_I(8) &= g_8\sqrt{2}\,(\bar{u},\bar{d},\bar{s})\begin{pmatrix} \frac{\pi^0}{\sqrt{2}}+\frac{\eta_8}{\sqrt{6}} & \pi^+ & K^+ \\ \pi^- & \frac{\pi^0}{\sqrt{2}}+\frac{\eta_8}{\sqrt{6}} & K^0 \\ K^- & \bar{K}^0 & -\frac{2\eta_8}{\sqrt{6}} \end{pmatrix}\begin{pmatrix} u \\ d \\ s \end{pmatrix} \\ &= g_8\left[\bar{n}(\boldsymbol{\tau}\cdot\boldsymbol{\pi})n+\sqrt{2}\,((\bar{n}\cdot K)s+\bar{s}(\bar{K}\cdot n))+\frac{1}{\sqrt{3}}(\bar{n}\,n)\eta_8-\frac{2}{\sqrt{3}}(\bar{s}s)\eta_8\right] \\ &= g_{nn\pi}\,\bar{n}(\boldsymbol{\tau}\cdot\boldsymbol{\pi})n+g_{snK}\,((\bar{n}\cdot K)s+\bar{s}(\bar{K}\cdot n))+g_{nn\eta}(\bar{n}n)\eta_8+g_{ss\eta}(\bar{s}s)\,\eta_8. \end{aligned} \tag{8.8}$$

Here, we introduced the isospin-basis couplings

$$g_{nn\pi}=g_8\,,\;g_{snk}=\sqrt{2}g_8\,,\;g_{nn\eta}=\frac{1}{\sqrt{3}}g_8\,,\;g_{ss\eta}=-\frac{2}{\sqrt{3}}g_8. \tag{8.9}$$

These couplings are similar to the OBE-couplings in baryon-baryon, and convenient for the transcription of the OBE-potentials from baryon-baryon to quark-quark.
The precise connection with the couplings of ESC models is given in Appendix B, where the (g_8, g_1) are defined in the framework of the quark-pair-creation (QPC) model. Furthermore, the connection between QQM-couplings in the constituent quark-model (CQM) and the BBM-couplings gives a direct determination of the QQM-couplings from the NN and YN data fitting.
For the numerical evaluation of the TME and MPE potentials we use the cartesian-octet presentation, see below.

C. Cartesian-octet Representation

For the numerical evaluation of the TME and MPE diagrams the cartesian-octet presentation is very convenient. The particle states created by the field operators are given in Table VIII C [51]. Here also the annihilation operators corresponding to the pseudo-scalar $SU(3)$ octet-representation $\{8\}$ are given in terms of the cartesian octet fields. For the pseudo-scalar mesons these are denoted by $\phi_i (i = 1, 2, \ldots, 8)$ [51, 52]. Similar expressions hold for the vector, axial-vector, and scalar mesons. The connection between the matrix-representation (8.5) and the cartesian-octet representation is

$$P^a_b=\frac{1}{\sqrt{2}}\sum_{i=1}^{8}(\lambda_i)_{ab}\phi_i\,,\phi_i=\frac{1}{\sqrt{2}}\sum_{a,b=1}^{3}(\lambda_i)_{ab}P^a_b \tag{8.10}$$

where $\lambda_i, i = 1, 8$ are the Gell-Mann matrices [51, 52], and where the indices $(a, b = 1, 2, 3)$. Similar expressions hold for the vector-, scalar-, and axial-mesons. The Gell-Mann matrices satisfy the the following commutation and anti-commutation relations

$$\left[\lambda_i,\lambda_j\right]=2if_{ijk}\,\lambda_k,\{\lambda_i,\lambda_j\}=\frac{4}{3}\delta_{ij}+2d_{ijk}\,\lambda_k\,. \tag{8.11}$$

where f_{ijk} are the totally anti-symmetric $SU(3)$-structure constants, and d_{ijk} are the totally symmetric constants.
The quark-quark matrix elements can now be computed using the cartesian octet states

$$\langle Q_3,Q_4|M|Q_1,Q_2\rangle=C^*_{3j}C^*_{4n}\,M(j,n;i,m)\,C_{1i}C_{2m}\,, \tag{8.12}$$

$\|\pi^+\rangle$	$= -\pi^{+\dagger}\|0\rangle$	π^+	$= \frac{1}{\sqrt{2}}(\phi_1 - i\phi_2)$
$\|\pi^-\rangle$	$= \pi^{-\dagger}\|0\rangle$	π^-	$= \frac{1}{\sqrt{2}}(\phi_1 + i\phi_2)$
$\|\pi^0\rangle$	$= \pi^{0\dagger}\|0\rangle$	π^0	$= \phi_3$
$\|K^+\rangle$	$= K^{+\dagger}\|0\rangle$	K^+	$= \frac{1}{\sqrt{2}}(\phi_4 - i\phi_5)$
$\|K^0\rangle$	$= K^{0\dagger}\|0\rangle$	K^0	$= \frac{1}{\sqrt{2}}(\phi_6 - i\phi_7)$
$\|K^-\rangle$	$= K^{-\dagger}\|0\rangle$	K^-	$= \frac{1}{\sqrt{2}}(\phi_4 + i\phi_5)$
$\|\bar{K}^0\rangle$	$= \bar{K}^{0\dagger}\|0\rangle$	$\bar{K}^0$	$= \frac{1}{\sqrt{2}}(\phi_6 + i\phi_7)$
$\|\eta_8\rangle$	$= \eta_8^\dagger\|0\rangle$	η	$= \phi_8$

TABLE I: Octet Representation Mesons States and Fields.

where C-coefficients relate the particle states to the cartesian states, see Table VIII C, and $M(j,n;i,m)$ depends on the structure of the graph. Below, we work out the M-operator for OBE-, TME-, and MPE-graphs in the cartesian-octet representation. Then, the physical two-baryon matrix elements in (8.12) can be obtained easily.

D. Computations for OBE-, TME-graphs SU(3)-factors

• **One-Boson-Exchange**: The $SU(3)$ matrix element for the OBE-graph Fig. 2 is given by

$$M_{obe}(j,n;i,m) = \sum_p{}' H_1^{(a)}(j,i;p)\, H_2^{(a)}(n,m;p)\,, \tag{8.13}$$

where $a = P, V, A, S$ and

$$H_a(j,i;p) \;=\; g_8^{(a)}\,\lambda_{ji}^{(p)} + \frac{g_1^{(a)}}{\sqrt{6}}\delta_{ji}\delta_{p9}. \tag{8.14}$$

The summation over p determines which mesons contribute to (8.14), and the prime indicates that one may restrict this summation in order to pick out a particular meson. This is in general necessary because within an $SU(3)$ nonet the mesons have different masses, and we need their couplings separately for a proper calculation of the potentials.

To illustrate this method of computation we consider π-exchange in the quark charge-exchange

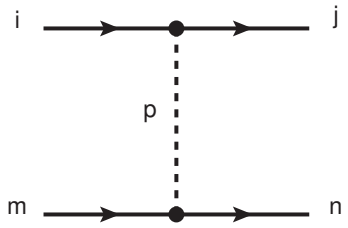

FIG. 2: Octet representation indices OBE-graphs. The solid lines denote quarks with labels i, m, j, n. The dashed lines with label p refers to the bosons: pseudo-scalar, vector, axial-vector, or scalar mesons.

reaction $U + D \to D + U$. We have for the isospin matrix element

$$\begin{aligned}\langle d,u|M_\pi|u,d\rangle &= \sum_{i,j,m,n=1}^{8}\sum_{p=1}^{3}\langle d|q_j\rangle\langle u|q_n\rangle\langle q_jq_n|M_\pi|q_iq_m\rangle\cdot\\ \times\langle q_i|u\rangle\langle q_m|d\rangle &= \sum_{i,j,m,n=1}^{8}\sum_{p=1}^{3}\delta_{2j}\delta_{1n}\delta_{i1}\delta_{m2}\cdot\\ \times\left\{g_8\lambda_{ji}^{(p)}\right\}&\left\{g_8\lambda_{nm}^{(p)}\right\} = 2g_8^2. \end{aligned} \tag{8.15}$$

Similarly, one gets $\langle d,u|M_\pi|u,d\rangle = -g_a^2$, which combined with (8.15) gives for the I=0 UD-state $-3g_a^2$, as expected.

• **Two-Meson-Exchange**: The $SU(3)$ matrix elements for the parallel (//) and crossed (X) TME-graphs Fig. 3 and Fig. 4 are given by

$$\begin{aligned} M_{tme}^{(//)}(j,n;i,m) &= {\sum_{p,q,r,s}}' H_2(j,r;q)\,H_1(r,i;p)\\ &\times\ H_2(n,s;q)\,H_1(s,m;p) \end{aligned} \tag{8.16}$$

$$\begin{aligned} M_{tme}^{(X)}(j,n;i,m) &= {\sum_{p,q,r,s}}' H_2(j,r;q)\,H_1(r,i;p)\\ &\times\ H_1(n,s;q)\,H_2(s,m;p) \end{aligned} \tag{8.17}$$

Again, like in the OBE-case, the numerical values of the $SU(3)$ matrix elements for TME can be computed easily making a computer program.

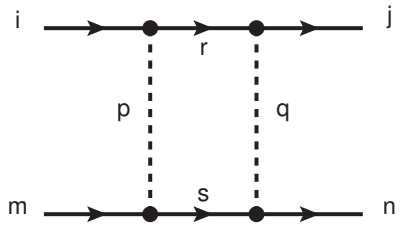

FIG. 3: Octet representation indices TME-parallel-graphs. The solid lines denote quarks with labels i, m, j, n, r, s. The dashed lines with labels p, q refers to the pseudo-scalar mesons.

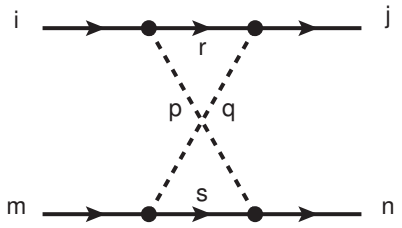

FIG. 4: Octet representation indices TME-crossed-graphs. The solid lines denote quarks with labels i, m, j, n, r, s. The dashed lines with labels p, q refers to the pseudo-scalar mesons.

IX. MPE INTERACTIONS AND $SU(3)$

A. Pair Couplings and $SU(3)$-symmetry

The $SU(3)$ octet and singlet mesons, denoted by the subscript 8 respectively 1, are in terms of the physical ones defined as follows:

(i) Pseudo-scalar-mesons:

$$\begin{aligned} \eta_1 &= \cos\theta_{PV}\eta' - \sin\theta_{PV}\eta \\ \eta_8 &= \sin\theta_{PV}\eta' + \cos\theta_{PV}\eta \end{aligned}$$

Here, η' and η are the physical pseudo-scalar mesons $\eta(957)$ respectively $\eta(548)$.

(ii) Vector-mesons:

$$\begin{aligned} \phi_1 &= \cos\theta_V\omega - \sin\theta_V\phi \\ \phi_8 &= \sin\theta_V\omega + \cos\theta_V\phi \end{aligned}$$

Here, ϕ and ω are the physical vector mesons $\phi(1019)$ respectively $\omega(783)$.

Similarly for the scalar and axial-vector mesons. The meson mixing angles are given in Ref. [10] Table IV. The $SU(3)$-invariant pair-interaction Hamiltonians is given in Ref. [36] section III.

B. Computations MPE-graphs SU(3)-factors

The $SU(3)$ matrix elements for the graphs with meson-pair vertices, the so-called MPE-graphs Fig. 5 and Fig. 6 are, using the cartesian-octet representation in section VIII C, given by

$$\begin{aligned} M_{(1-pair)}(j,n;i,m) &= \sum_{p,q,r,s}{}' H_{pair}(j,i,s)\, O(q,p,s) \\ &\times H_2(m,r,q)\, H_1(r,m,p) \end{aligned} \tag{9.1}$$

$$\begin{aligned} M_{(2-pair)}(j,n;i,m) &= \sum_{p,q,r,s=1}{}' H_{pair}(j,i,s)\, O(q,p,s) \\ &\times O(q,p,r)\, H_{pair}(n,m,p) \end{aligned} \tag{9.2}$$

Again, like in the OBE-case, the numerical values of the $SU(3)$ matrix elements for MPE can be computed straightforwardly making a computer program.

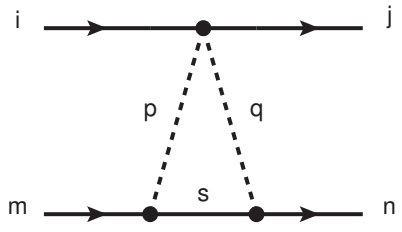

FIG. 5: Octet representation indices MPE one-pair-graphs. The solid lines denote quarks with labels i, m, j, n, s. The dashed lines with labels p, q refers to the pseudo-scalar etc. mesons.

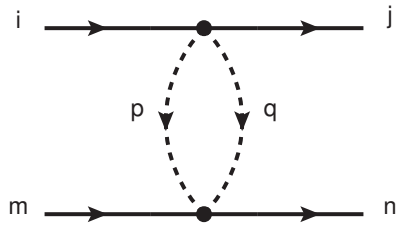

FIG. 6: Octet representation indices MPE two-pair-graphs. The solid lines denote quarks with labels i, m, j, n. The dashed lines with labels p, q refers to the pseudo-scalar etc. mesons.

C. Form Factors

Also in this work, like in the NSC97-models [53], the form factors depend on the SU(3) assignment of the mesons, In principle, we introduce form factor masses Λ_8 and Λ_1 for the {8} and {1} members of each meson nonet, respectively. In the application to YN and YY, we allow for SU(3)-breaking, by using different cut-offs for the strange mesons K, K^*, and κ. Moreover, for the $I = 0$-mesons we assign the cut-offs as if there were no meson-mixing. For example we assign Λ_1 for η', ω, ϵ, and Λ_8 for η, ϕ, S^*, etc.

X. RELATION QQM- AND BBM-COUPLINGS

In [1] the relation between the QQM- and BBM-couplings is determined by requiring that the 1/M-expansion of the baryon-baryon potentials is reproduced by folding, using the SU(6) quark-model [3]. The relations are

(a) Pseudoscalar mesons:

$$f^p_{QQ\pi} = f^P_{BB\pi}, \tag{10.1}$$

and similar relations for the η, K, η'. This follows from $g^p_{QQ\pi} = g^p_{BB\pi}/3$ and $m_q = M_B/3$.

(b) Vector mesons:

$$g^v_{QQ\rho} = \frac{1}{3} g^V_{BB\rho}\ ,\ f^v_{QQ\rho} = \frac{1}{3} f^V_{BB\rho}, \tag{10.2}$$

and similar relations for ϕ, K^*, ω.

(c) Scalar mesons:

$$g^s_{QQa_0} = \frac{1}{3} g^S_{BBa_0}, \tag{10.3}$$

and similar relations for $f_0(993), \kappa, \epsilon = f_0(620)$.

(d) Axial-vector mesons (I):

$$g^a_{QQA_1} = \frac{1}{3} g^A_{BBA_1}\ ,\ f^a_{QQA_1} = \frac{1}{3} f^A_{BBA_1}, \tag{10.4}$$

and similar relations for $D_1(1285)$, $K_A(1336)$, $E_1(1420)$.

(e) Axial-vector mesons (II):

$$f^b_{QQB_1} = \frac{1}{3} f^B_{BBB_1}, \tag{10.5}$$

and similar relations for $D_1(1285)$, $K_B(1300)$, and $E_1(1420)$.

(f) Diffractive exchanges: Under the usual assumption of the quark-additivity of the pomeron couplings [4] one has $g_{QQP} = g_{NNP}/3$, and similarly for the odderon couplings.

XI. GLUON AND CONFINING POTENTIALS

The one gluon-exchange (OGE) has the form

$$V_{OGE} = A\ (\boldsymbol{\lambda}_1 \cdot \boldsymbol{\lambda}_2)\ V_V(m_G, r, \Lambda_G), \tag{11.1}$$

S	I	C	$\langle \lambda_1 \cdot \lambda_2 \rangle$	$\langle \sigma_1 \cdot \sigma_2 \rangle$
0	0	{3*}	-8/3	-3
0	1	{6}	+4/3	-3
1	0	{6}	+4/3	+1
1	1	{3*}	-8/3	+1

TABLE II: Color and Spin matrix elements, $\mathbf{F} = \lambda/2$.

where V_V is the OBE vector exchange potential. Here, $m_G = 480$ MeV, which is the mass of the gluon propagator in the "liquid instanton model" [54]. In [55, 56] the confining potential is taken to be a scalar color-octet exchange potential. In [57] the confining potential is color-singlet scalar exchange of the form

$$V_{conf} = C_0 + C_1 \, (\lambda_1 \cdot \lambda_2) \, r^2, \tag{11.2}$$

where C_0 is adjusted to give the 939 MeV for the nucleon mass, and depends on the other parts of the total Q-Q potential. For the GBE-model [18, 58] in [57] table III the fitted GBE parameters are C_0= -416 MeV, C_1= 2.33.
Since the GBE-model approach is also that of Manohar-Georgi, we choose in this work the confining potential in (11.2).

XII. SU(3) NJL-FORM INSTANTON POTENTIALS

For SU(2) with $\psi = (u, d)$ and $\tau_0 = \mathbf{1}$, the 't Hooft quark-quark interaction reads

$$\mathcal{L}_{ud} = G_I \Big[(\bar{\psi}\tau_0\psi)^2 + (\bar{\psi} i\gamma_5 \tau\psi)^2 - (\bar{\psi}\tau\psi)^2 - (\bar{\psi} i\gamma_5 \tau_0\psi)^2 \Big], \tag{12.1}$$

The SU(3) generalization of the 't Hooft interaction for the (u,d,s) quarks in the NJL-form reads

$$\mathcal{L}_{uds} = G_I \Big[(\bar{\psi}\lambda_0\psi)^2 + (\bar{\psi} i\gamma_5 \lambda\psi)^2 - (\bar{\psi}\lambda\psi)^2 - (\bar{\psi} i\gamma_5 \lambda_0\psi)^2 \Big], \tag{12.2}$$

with $G_I = \lambda_{ud}/4$, and where $\psi = (u, d, s)$ i.e. the flavor {3}-irrep spinor field, $\lambda_0 = \sqrt{4/3}\ \mathbf{1}$, and $\lambda_a, a = 1, 8$ are the Gell-Mann matrices.

1. Diagonal Potentials: Working out the diagonal terms we have

$$\mathcal{L}_{uds} \Rightarrow G_I (\lambda_{0,1}\lambda_{0,2} - \lambda_1 \cdot \lambda_2) \Big[(\bar{q}_i q_i)^2 + (\bar{q}_i \gamma_5 q_i)^2 \Big],$$

with i=u,d,s. In the CM-system assigning the momenta $(\mathbf{p}, -\mathbf{p})$ in the initial state and $(\mathbf{p}', -\mathbf{p}')$ in the final state one has

$$\begin{aligned} (\bar{q}q)^2 \ &\rightarrow \ 1 - \frac{1}{4M^2}[2\mathbf{p}' \cdot \mathbf{p} + i(\sigma_1 + \sigma_2) \cdot \mathbf{p}' \times \mathbf{p}], \\ (\bar{q}\gamma_5 q)^2 \ &\rightarrow \ -\frac{1}{4M^2} \, \sigma_1 \cdot (\mathbf{p}' - \mathbf{p}) \, \sigma_2 \cdot (\mathbf{p}' - \mathbf{p}) \end{aligned}$$

Using the variables $\mathbf{k} = \mathbf{p}' - \mathbf{p}$ and $\mathbf{q} = (\mathbf{p}' + \mathbf{p})/2$ the potential becomes

$$\widetilde{V}(\mathbf{p}',\mathbf{p}) = -2G_I\left(\lambda_{0,1}\lambda_{0,2} - \boldsymbol{\lambda}_1\cdot\boldsymbol{\lambda}_2\right)\Big[1+\left(1-\frac{1}{3}\boldsymbol{\sigma}_1\cdot\boldsymbol{\sigma}_2\right)\frac{\mathbf{k}^2}{4M^2} - \frac{\mathbf{q}^2+\mathbf{k}^2/4}{2M^2}$$
$$-\frac{1}{4M^2}\left(\boldsymbol{\sigma}_1\cdot\mathbf{k}\boldsymbol{\sigma}_2\cdot\mathbf{k} - \frac{1}{3}\boldsymbol{\sigma}_1\cdot\boldsymbol{\sigma}_2\,\mathbf{k}^2\right) + \frac{i}{4M^2}(\boldsymbol{\sigma}_1+\boldsymbol{\sigma}_2)\cdot\mathbf{n} + \frac{1}{16M^4}(\boldsymbol{\sigma}_1\cdot\mathbf{n})(\boldsymbol{\sigma}_2\cdot\mathbf{n})\Big], \tag{12.3}$$

where $\mathbf{n} = \mathbf{q}\times\mathbf{k}$, and the quadratic-spin-orbit term is added for completenes.
Adding a gaussian cut-off $F_I(\mathbf{k}^2) = \exp\big[-\mathbf{k}^2/(\Lambda^2\big]$, with $m_I = \Lambda/2$, the local instanton potentials become, apart from the flavor factor,

$$V_I = -\frac{2g_I}{\pi\sqrt{\pi}}\frac{m_I^3}{\Lambda^2}\Big[1+\frac{m_I^2}{2M^2}\left(3-2m_I^2r^2\right)\left(1-\frac{1}{3}\boldsymbol{\sigma}_1\cdot\boldsymbol{\sigma}_2\right) + \frac{m_I^2}{3M^2}\,(m_Ir)^2\,S_{12}$$
$$+\frac{m_I^2}{M^2}\,\mathbf{L}\cdot\mathbf{S} + \frac{m_I^4}{M^4}\,Q_{12}\Big]\,\exp[-m_I^2r^2]. \tag{12.4}$$

Taking $\Lambda = 1$ GeV/c^2, $G_I = \lambda_{ud}/4$ the coupling $g_I = G_I\Lambda^2 = 2.0-2.5$.

For u,d quarks the flavor factor becomes, see also (2.1), $(1-\boldsymbol{\tau}_1\cdot\boldsymbol{\tau}_2)$, which gives 0 and 4 for I=1 and I=0 respectively. For $m_I = 200$ MeV and $M = m_Q = M_N/3 \approx 315$ MeV, the factor $(1+3m_I^2/2M^2) \approx 1.6$. This gives $V_I(^1S_0, I=1) = 0$ and $V_I(^3S_1, I=0) < 0$ for r=0.
In analyzing the U(1)-problem, Weinberg [19] chooses $\lambda_0 = \sqrt{2/3}\,\mathbf{1}$ giving for u,d quarks $(1/3-\boldsymbol{\tau}_1\cdot\boldsymbol{\tau}_2)$ which is -2/3 and 10/3 for I=1 and I=0 respectively. This gives repulsion and attraction for respectively $^1S_0(I=1)$ and $^3S_1(I=0)$.
The non-local term in (12.3) has the same sign as for scalar and vector exchange, and opposite to Pomeron exchange. Therefore, compare [39] formula (34), one has

$$V_{n.l.}(r) = -G_I\left\{\boldsymbol{\nabla}^2\exp\Big[-\frac{1}{4}\Lambda^2r^2\Big] + \exp\Big[-\frac{1}{4}\Lambda^2r^2\Big]\boldsymbol{\nabla}^2\right\}$$
$$\equiv -\Big[\boldsymbol{\nabla}^2\frac{\phi(r)}{2M_{red}} + \frac{\phi(r)}{2M_{red}}\Big], \tag{12.5}$$

which, with $M_{red} = M/2$, gives

$$\phi(r) = +(G_IM^2)\left(\frac{\Lambda}{2\sqrt{\pi}M}\right)^3\,\exp\Big[-\frac{1}{4}\Lambda^2r^2\Big]. \tag{12.6}$$

Now, $(\Lambda/2\sqrt{\pi}M) \approx 0.85$ and 0.56 for the u,d and s quark respectively. For $g_I = G_IM^2 = 2.0-2.5$ the non-local function $\phi(r)$ is not small.
The flavor factor for the non-strange quarks becomes $(1-\boldsymbol{\tau}_1\cdot\boldsymbol{\tau}_2)$, which is due to the choice for λ_0.

2.1. Non-diagonal Potentials: There are no non-diagonal terms!? For example $s\to u$:

$$(\bar\psi\boldsymbol{\lambda}\psi)^2 \to (\bar\psi\lambda_4\psi)^2 + (\bar\psi\lambda_5\psi)^2 \to (\bar us)^2 - (\bar us)^2 = 0, etc.$$

XIII. ESC16-MODEL: FITTING $NN\oplus YN\oplus YY$-DATA

In the simultaneous χ^2-fit of the NN-, YN-, and YY-data a *single set of parameters* was used, which means the same parameters for all BB-channels. The input NN-data are the same as in Ref. [35], and we refer the reader to this paper for a description of the employed phase shift analysis [59, 60].

It appeared that the OBE-couplings could be constrained successfully by the 'naive' predictions of the QPC-model [3, 5]. Although these predictions, see section V, are 'bare' ones, the policy was to keep the many OBE-couplings in the neighborhood of the QPC-values. Also, it appeared that we could either fix the $F/(F+D)$-ratios to those as suggested by the QPC-model, or apply the same restraining strategy as for the OBE-couplings.

A. Fitted BB-parameters

The treatment of the broad mesons ρ and ϵ was similar to that in the OBE-models [39, 40]. For the ρ-meson the same parameters are used as in these references. However, for the $\epsilon = f_0(620)$ assuming $m_\epsilon = 620$ MeV and $\Gamma_\epsilon = 464$ MeV the Bryan-Gersten parameters [61] are used. For the chosen mass and width they are: $m_1 = 496.39796$ MeV, $m_2 = 1365.59411$ MeV, and $\beta_1 = 0.21781, \beta_2 = 0.78219$. Other meson masses are given in Table XIII B. The sensitivity for the values of the cut-off masses of the η and η' is very weak. Therefore we have set the {1}-cut-off imass for the pseudoscalar nonet equal to that for the {8}. Likewise, for the two nonets of the axial-vector mesons, see table XIII B.

Summarizing the parameters for baryon-baryon (BB) are:
(i) NN Meson-couplings: $f_{NN\pi}, f_{NN\eta'}$, $g_{NN\rho}, g_{NN\omega}$, $f_{NN\rho}, f_{NN\omega}$, $g_{NNa_0}, g_{NN\epsilon}$, g_{NNa_1}, f_{NNa_1}, $g_{NNf_1'}$, $f_{NNf_1'}, f_{NNb_1}, f_{NNh_1'}$
(ii) $F/(F+D)$-ratios: α_V^m, α_A
(iii) NN Pair couplings: $g_{NN(\pi\pi)_1}, f_{NN(\pi\pi)_1}, g_{NN(\pi\rho)_1}, g_{NN\pi\omega}, g_{NN\pi\eta}, g_{NN\pi\epsilon}$
(iv) Diffractive couplings and masslike parameters $g_{NNP}, g_{NNO}, f_{NNO}, m_P, m_O$
(v) Cut-off masses: $\Lambda_8^P = \Lambda_1^P, \Lambda_8^V, \Lambda_1^V, \Lambda_8^S, \Lambda_1^S$, and $\Lambda_8^A = \Lambda_1^A$.

The pair coupling $g_{NN(\pi\pi)_0}$ was kept fixed at zero. Note that in the interaction Hamiltonians of the pair-couplings (7.15) the partial derivatives are scaled by m_π, and there is a scaling mass M_N.

The ESC models, are fully consistent with $SU(3)$-symmetry using a straightforward extension of the NN-model to YN and YY. This is the case for the OBE- and TPS-potentials, as well as for the Pair-potentials. All $F/(F+D)$-ratio's are taken as fixed with heavy-meson saturation in mind.

B. Coupling Constants, $F/(F+D)$ Ratios, and Mixing Angles

In Table XIII B we give the ESC16 meson masses, and the fitted couplings and cut-off parameters [9, 10]. Note that the axial-vector couplings for the B-mesons are scaled with m_{B_1}. The mixing for the pseudo-scalar, vector, and scalar mesons, as well as the handling of the diffractive potentials, has been described elsewhere, see e.g. Refs. [40, 53]. The mixing scheme of the axial-vector mesons is completely similar as for the vector etc. mesons, except for the mixing angle. As mentioned above, we searched for solutions where all OBE-couplings are compatible with the QPC-predictions. This time the QPC-model contains a mixture of the $^3P_0$ and $^3S_1$ mechanism, whereas in Ref. [35] only the $^3P_0$-mechanism was considered. For the pair-couplings all $F/(F+D)$-ratios were fixed to the predictions of the QPC-model.

One notices that all the BBM α's have values rather close to that which are expected from the QPC-model. In the ESC16 solution $\alpha_A \approx 0.38$, which is close to $\alpha_A \sim 0.4$. As in previous works, e.g. Ref. [39], $\alpha_V^e = 1$ is kept fixed. Above, we remarked that the axial-nonet parameters may be sensitive to whether or not the heavy pseudoscalar nonet with the $\pi(1300)$ are included.

In Table XIII B we show the OBE-coupling constants and the gaussian cut-off's Λ. The used $\alpha =:$ $F/(F+D)$-ratio's for the OBE-couplings are: pseudo-scalar mesons $\alpha_{ps} = 0.365$, vector mesons $\alpha_V^e = 1.0, \alpha_V^m = 0.472$, and scalar-mesons $\alpha_S = 1.00$, which is calculated using the physical $S^* =: f_0(993)$ coupling etc..

In Table XIII B we list the fitted Pair-couplings for the MPE-potentials. We recall that only One-pair graphs are included, in order to avoid double counting, see Ref. [35]. The $F/(F+D)$-ratios are all fixed,

meson	mass	$g/\sqrt{4\pi}$	$f/\sqrt{4\pi}$	Λ
π	138.04		0.2684	1030.96
η	547.45		0.1368*	,,
η'	957.75		0.3181	,,
ρ	768.10	0.5793	3.7791	680.79
ϕ	1019.41	–1.2384*	2.8878*	,,
ω	781.95	3.1149	–0.5710	734.21
a_1	1270.00	–0.8172	–1.6521	1034.13
f_1	1420.00	0.5147	4.4754	,,
f_1'	1285.00	–0.7596	–4.4179	,,
b_1	1235.00		–2.2598	1030.96
h_1	1380.00		–0.0830*	,,
h_1'	1170.00		–1.2386	,,
a_0	962.00	0.5393		830.42
f_0	993.00	–1.5766*		,,
ε	620.00	2.9773		1220.28
Pomeron	212.06	2.7191		
Odderon	268.81	4.1637	–3.8859	

TABLE III: Meson couplings and parameters employed in the ESC16-potentials. Coupling constants are at $\mathbf{k}^2 = 0$. An asterisk denotes that the coupling constant is constrained via SU(3). The masses and Λ's are given in MeV.

J^{PC}	$SU(3)$-irrep	$(\alpha\beta)$	$g/4\pi$	$F/(F+D)$
0^{++}	$\{1\}$	$g(\pi\pi)_0$	—	—
0^{++}	,,	$g(\sigma\sigma)$	—	—
0^{++}	$\{8\}_s$	$g(\pi\eta)$	-0.6894	1.000
1^{--}	$\{8\}_a$	$g(\pi\pi)_1$	0.2519	1.000
		$f(\pi\pi)_1$	–1.7762	0.400
1^{++}	,,	$g(\pi\rho)_1$	5.7017	0.400
1^{++}	,,	$g(\pi\sigma)$	–0.3899	0.400
1^{++}	,,	$g(\pi P)$	—	—
1^{+-}	$\{8\}_s$	$g(\pi\omega)$	–0.3287	0.365

TABLE IV: Pair-meson coupling constants employed in the ESC16 MPE-potentials. Coupling constants are at $\mathbf{k}^2 = 0$. The F/(F+D)-ratio are QPC-predictions, except that $\alpha_{(\pi\omega)} = \alpha_P$, which is very close to QPC.

assuming heavy-boson domination of the pair-vertices. The ratios are taken from the QPC-model for $Q\bar{Q}$-systems with the same quantum numbers as the dominating boson. For example, the α-parameter for the axial $(\pi\rho)_1$-pair could fixed at the quark-model prediction 0.40, see Table XIII B. The BB-Pair couplings are calculated, assuming unbroken $SU(3)$-symmetry, from the NN-Pair coupling and the $F/(F+D)$-ratio using $SU(3)$. So, in addition to the 14 parameters used in Ref. [62] we now have 6 pair-coupling fit parameters. In Table XIII B the fitted pair-couplings are given. The $(\pi\rho)_1$-coupling is large as expected from A_1-saturation, see Ref. [62]. In Table XIII B we show the MPE-coupling constants. The used $\alpha =: F/(F+D)$-ratio's for the MPE-couplings are: $(\pi\eta)$ pairs $\alpha(\{8_s\}) = 1.0$, $(\pi\pi)_1$ pairs $\alpha_V^e(\{8\}_a) = 1.0, \alpha_V^m(\{8\}_a) = 0.400$, and the $(\pi\rho)_1$ pairs $\alpha_A(\{8\}_a) = 0.400$. The $(\pi\omega)$ pairs $\alpha(\{8_s\})$ has been set equal to $\alpha_{pv} = 0.365$.

Assuming heavy-meson dominance of the meson-pair couplings, similarly to the QQM-couplings all QQ meson-pair couplings get a factor 1/3, i.e. $g_{QQm_1m_2} = G_{BBm_1m_2}/3$.

In Tables XIII B, XIII B and XIII B the NN, QN, and QQ phases are shown respectively. This for the complete ESC16 model with NN parameters **parbbsc.new17def2**. *The scale parameters for the QQM-couplings and quark mass are both 1/3. The gluon mass* $m_{glu} = 420$ *MeV/c*^{2}*, the QQM form factor cut-off is set to* $\Lambda_{QQM} = 986.6$ *MeV/c*^{2}*, and furthermore the confinement potential is left out.*
Note: the extra couplings for the QQM-vertex w.r.t. the NNM-couplings are set to zero.

$T_{\rm lab}$	0.38	1	5	10	25	50	100	150	215	320
$^1S_0(np)$	54.57	62.02	63.47	59.72	50.48	39.82	25.45	15.11	4.65	−8.34
$^1S_0$	14.62	32.62	54.75	55.16	48.67	38.97	25.06	14.85	4.44	−8.53
$^3S_1$	159.39	147.77	118.25	102.72	80.81	63.03	43.62	31.27	19.58	5.83
ϵ_1	0.03	0.11	0.68	1.17	1.82	2.15	2.50	2.94	3.64	4.93
$^3P_0$	0.02	0.14	1.61	3.81	8.81	11.80	9.68	4.83	−1.86	−11.73
$^3P_1$	−0.01	−0.08	−0.89	−2.04	−4.89	−8.29	−13.28	−17.35	−21.87	−27.90
$^1P_1$	−0.05	−0.19	−1.50	−3.07	−6.39	−9.81	−14.65	−18.75	−23.38	−29.44
$^3P_2$	0.00	0.02	0.22	0.67	2.51	5.80	10.90	14.04	16.24	17.07
ϵ_2	−0.00	−0.00	−0.05	−0.20	−0.81	−1.71	−2.71	−2.99	−2.84	−2.18
$^3D_1$	−0.00	−0.01	−0.18	−0.68	−2.83	−6.51	−12.40	−16.69	−20.72	−25.04
$^3D_2$	0.00	0.01	0.22	0.85	3.70	8.93	17.22	22.15	24.99	25.05
$^1D_2$	0.00	0.00	0.04	0.17	0.69	1.70	3.78	5.70	7.64	9.20
$^3D_3$	0.00	0.00	0.00	0.00	0.03	0.24	1.17	2.31	3.61	4.86
ϵ_3	0.00	0.00	0.01	0.08	0.55	1.59	3.46	4.81	5.97	6.99
$^3F_2$	0.00	0.00	0.00	0.01	0.11	0.34	0.80	1.10	1.14	0.39
$^3F_3$	−0.00	−0.00	−0.01	−0.03	−0.23	−0.67	−1.46	−2.06	−2.66	−3.50
$^1F_3$	−0.00	−0.00	−0.01	−0.06	−0.41	−1.10	−2.11	−2.77	−3.46	−4.69
$^3F_4$	0.00	0.00	0.00	0.00	0.02	0.12	0.51	1.04	1.80	3.00
ϵ_4	−0.00	−0.00	−0.00	−0.00	−0.05	−0.19	−0.53	−0.83	−1.13	−1.46
$^3G_3$	−0.00	−0.00	−0.00	−0.00	−0.05	−0.26	−0.93	−1.73	−2.77	−4.17
$^3G_4$	0.00	0.00	0.00	0.01	0.17	0.71	2.11	3.52	5.17	7.28
$^1G_4$	0.00	0.00	0.00	0.00	0.04	0.15	0.41	0.69	1.06	1.70
$^3G_5$	−0.00	−0.00	−0.00	−0.00	−0.01	−0.05	−0.16	−0.25	−0.28	−0.19
ϵ_5	0.00	0.00	0.00	0.00	0.04	0.20	0.70	1.22	1.83	2.62

TABLE V: Nucleon-Nucleon ESC16 nuclear-bar *PP* and *NP* phases in degrees.

XIV. SUMMARY AND OUTLOOK

The ESC-approach to the baryon-baryon interactions is able to make a connection between the available baryon-baryon data on the one hand, and on the other hand the underlying quark structure of the baryons and mesons. Namely, a succesfull description of both the *NN*- and *YN*-scattering data is obtained with meson-baryon coupling parameters which are almost all explained by the QPC-model, which implicitly makes use of the CQM. The finding that in the CQM it is possible to derive the ESC baryon-baryon meson-exchange potentials from meson-exchange between quarks via folding with the ground-state baryon quark wave functions opens the way to derive meson-exchange quark-quark potentials almost parameter free.

The method followed in this paper is based on these observations. The potentials are worked out in a $1/m_Q$-expansion. For quark masses significantly smaller than the constituent quarks the Kadyshevsky formalism in momentum space provides a suitable framework for relativistic calculations. In

$T_{\rm lab}$	0.38	1	5	10	25	50	100	150	215	320
$^1S_0(np)$	0.288	0.445	0.727	0.648	−0.254	−2.278	−6.443	−10.293	−14.761	−20.894
$^1S_0$	0.194	0.364	0.700	0.650	−2135	−2.207	−6.348	−10.192	−14.661	−20.804
$^3S_1$	0.544	0.855	1.614	1.865	1.559	0.828	−2.159	−6.54	−10.52	−16.09
ϵ_1	0.007	0.030	0.260	0.568	1.254	1.828	2.159	2.153	2.021	1.765
$^3P_0$	0.003	0.015	0.163	0.379	0.885	1.230	0.926	0.052	−1.435	−4.205
$^3P_1$	−0.002	−0.011	−0.120	−0.283	−0.707	−1.180	−1.677	−1.922	−2.159	−2.699
$^1P_1$	−0.000	−0.000	−0.000	−0.393	−0.830	−1.141	−1.174	−0.964	−0.680	−0.568
$^3P_2$	0.000	0.002	0.029	0.085	0.333	0.857	1.977	2.990	3.985	4.720
ϵ_2	−0.000	−0.000	−0.005	−0.020	−0.089	−0.203	−0.346	−0.402	−0.395	−0.282
$^3D_1$	−0.000	−0.000	−0.010	−0.042	−0.210	−0.515	−0.864	−0.871	−0.567	0.190
$^3D_2$	0.000	0.000	0.000	0.000	0.000	0.893	1.755	2.343	2.806	3.068
$^1D_2$	0.000	0.000	0.000	0.000	0.000	0.201	0.468	0.741	1.068	1.443
$^3D_3$	0.000	0.000	0.000	0.000	0.000	0.000	0.000	0.233	0.538	1.161
ϵ_3	0.000	0.000	0.000	0.000	0.000	0.000	0.000	0.583	0.721	0.796
$^3F_2$	0.000	0.000	0.000	0.000	0.000	0.033	0.076	0.086	0.042	−0.121
$^3F_3$	0.000	0.000	0.000	0.000	0.000	- 0.000	0.000	−0.281	−0.371	−0.442
$^1F_3$	−0.000	−0.000	−0.000	−0.000	−0.000	−0.000	−0.000	−0.410	−0.543	−0.728
$^3F_4$	0.000	0.000	0.000	0.000	0.000	0.000	0.000	0.000	0.127	0.233
ϵ_4	−0.000	−0.000	−0.000	−0.000	−0.000	−0.000	−0.000	−0.000	−0.129	−0.165
$^3G_3$	−0.000	−0.000	−0.000	−0.000	−0.000	−0.000	−0.000	−0.142	−0.199	−0.213
$^3G_4$	0.000	0.000	0.000	0.000	0.000	0.000	0.000	0.000	0.000	0.728
$^1G_4$	0.000	0.000	0.000	0.000	0.000	0.000	0.000	0.000	0.112	0.179
$^3G_5$	−0.000	−0.000	−0.000	−0.000	−0.000	−0.000	−0.000	−0.000	−0.000	−0.000
ϵ_5	0.000	0.000	0.000	0.000	0.000	0.000	0.000	0.000	0.000	0.0000

TABLE VI: Quark-Nucleon ESC16 nuclear-bar *UP* and *DP* phases in degrees.

this case the $1/m_Q$-expansion can be avoided by using the complete formulas for the Kadyshevsky diagrams. This lowering of the quark mass will happen in dense quark-matter, and therefore a relativistic many-body theory is eventually needed. Similar to the Dirac-Bruckner Theory, the Kadyshevsky-Bethe-Goldstone equation for the G-matrix is obtained in momentum-space, which can be solved using standard methods.

The tables for the Quark-quark and Quark-nucleon phase shifts have some physical reality only for the hypothetical case of completely deconfined matter. They mainly serve to give an impression of the strength of the quark-quark and quark-nucleon interactions compared to the nucleon-nucleon interactions.

Application of this work, for example, can be the study of neutron-star (NS) matter modeled as a mixture of quark and baryon matter. The G-matrices of both kinds of matter are described with largely common parameters.

Finally, we mention the possibility to derive an ΩΩ-potential by folding the QQ-potentials with the Ω three-quark wave function.

$T_{\rm lab}$	0.38	1	5	10	25	50	100	150	215	320
$^1S_0(np)$	0.864	1.391	3.047	4.203	6.197	−7.869	−9.103	−9.182	−8.529	−6.686
$^1S_0$	1.099	2.168	5.665	8.144	12.452	16.147	19.268	20.221	20.155	18.781
$^3S_1$	0.688	1.109	2.440	3.384	5.071	−6.604	−7.982	−8.360	−8.115	-6.853
ϵ_1	0.001	0.002	0.024	0.060	0.175	0.338	0.569	0.733	0.900	1.123
$^3P_0$	0.001	0.004	0.050	0.142	5.25	1.330	3.106	4.805	6.688	8.847
$^3P_1$	0.000	0.001	0.010	0.033	0.152	0.473	1.382	2.466	3.964	6.328
$^1P_1$	−0.000	−0.000	−0.000	−0.035	−0.093	−0.156	−0.186	−0.145	−0.038	0.176
$^3P_2$	0.000	0.001	0.017	0.049	0.197	0.559	1.551	2.779	4.600	7.813
ϵ_2	−0.000	−0.000	−0.000	−0.001	−0.006	−0.021	−0.057	−0.096	−0.147	−0.213
$^3D_1$	−0.000	−0.000	−0.000	−0.002	−0.011	−0.036	−0.079	−0.088	−0.039	0.185
$^3D_2$	0.000	0.000	0.000	0.000	0.000	0.060	0.145	0.219	0.303	0.428
$^1D_2$	0.000	0.000	0.000	0.000	0.000	0.022	0.080	0.173	0.345	0.743
$^3D_3$	0.000	0.000	0.000	0.000	0.000	0.000	0.000	−0.026	−0.019	0.066
ϵ_3	0.000	0.000	0.000	0.000	0.000	0.000	0.000	0.050	0.073	0.099
$^3F_2$	0.000	0.000	0.000	0.000	0.000	0.003	0.016	0.043	0.106	0.280
$^3F_3$	0.000	0.000	0.000	0.000	0.000	- 0.000	0.000	−0.008	0.006	0.068
$^1F_3$	−0.000	−0.000	−0.000	−0.000	−0.000	−0.000	−0.000	−0.037	−0.052	−0.066
$^3F_4$	0.000	0.000	0.000	0.000	0.000	0.000	0.000	0.000	0.012	0.027
ϵ_4	−0.000	−0.000	−0.000	−0.000	−0.000	−0.000	−0.000	−0.000	−0.011	−0.018
$^3G_3$	−0.000	−0.000	−0.000	−0.000	−0.000	−0.000	−0.000	−0.008	−0.016	−0.031
$^3G_4$	0.000	0.000	0.000	0.000	0.000	0.000	0.000	0.000	0.000	0.053
$^1G_4$	0.000	0.000	0.000	0.000	0.000	0.000	0.000	0.000	0.010	0.019
$^3G_5$	0.000	0.000	0.000	0.000	0.000	0.000	0.000	0.000	0.000	0.000
ϵ_5	0.000	0.000	0.000	0.000	0.000	0.00R0	0.000	0.000	0.000	0.000

TABLE VII: Quark-Quark ESC16 nuclear-bar UU and DU phases in degrees.

	experimental data			ESC16
$a_{pp}(^1S_0)$	−7.828	±	0.008	−7.7718
$r_{pp}(^1S_0)$	2.800	±	0.020	2.7612*
$a_{np}(^1S_0)$	−23.748	±	0.010	−23.7346
$r_{np}(^1S_0)$	2.750	±	0.050	2.6992*
$a_{nn}(^1S_0)$	−18.63	±	0.48	−17.783
$r_{nn}(^1S_0)$	2.860	±	0.15	2.8301*
$a_{np}(^3S_1)$	5.424	±	0.004	5.4396*
$r_{np}(^3S_1)$	1.760	±	0.005	1.7488*
E_B	−2.224644	±	0.000046	−2.224636
Q_e	0.286	±	0.002	0.2727

TABLE VIII: ESC16 Low energy parameters: S-wave scattering lengths and effective ranges, deuteron binding energy E_B, and electric quadrupole Q_e. Experimental values and references, see [63]. The asterisk denotes that the low-energy parameters were not searched.

Appendix A: Kadyshevsky G-matrix Equation

In a fermi-system, *e.g.* quark matter, the Kadyshevsky-Bethe-Goldstone-Kadyshevsky equation (BGKE) is depicted in Fig. 7, and reads

$$\mathcal{F}(\mathbf{p}',\mathbf{p};W) = K(\mathbf{p}',\mathbf{p};W) + \frac{1}{(2\pi)^3}\int \frac{d^3p''}{2E(\mathbf{p}'')}\, K(\mathbf{p}',\mathbf{p}'';W)\ \cdot$$
$$\times\frac{M^2}{E(\mathbf{p}'')\,[E(\mathbf{p}'')-E(\mathbf{p})-i\epsilon]}\, Q_P[n_F(p'')]\,\mathcal{F}(\mathbf{p}'',\mathbf{p};W), \tag{A1}$$

which corresponds to Eq. (5.11). Then, the Bethe-Goldstone-Kadyshevsky two-particle wave function reads

$$\psi(p;W) = \psi^{(0)}(p) + \int \frac{d^3p''}{2E(\mathbf{p}'')(2\pi)^3}\cdot$$
$$\times\frac{M^2}{E(\mathbf{p}'')\,[E(\mathbf{p}'')-E(\mathbf{p})-i\epsilon]}\, Q_P[n_F(p'')]\,\psi(p'';W), \tag{A2}$$

where $\psi^{(0)}(p;W)$ corresponds to the two-particle plane-wave product state $|\phi_0(p_1)\rangle|\phi_0(p_2)\rangle$, with $P = p_1 + p_2, p = p_1 - p_2$, and $W = p_1^0 + p_2^0$. Here, $\phi^{(0)}(p)$ is the plane wave in the case of matter or a model wave function for finite nuclei.
Then, the corresponding G-matrix is introduced in the standard way by defining $\mathcal{G}(p;W) = \langle\psi^{(0)}|K_{op}\,|\psi(p;W)\rangle$, giving the equation

$$\mathcal{G}(\mathbf{p}',\mathbf{p};W) = K(\mathbf{p}',\mathbf{p};W) + \frac{1}{(2\pi)^3}\int \frac{d^3p''}{2E(\mathbf{p}'')}\, K(\mathbf{p}',\mathbf{p}'';W)\cdot$$
$$\times\frac{M^2}{E(\mathbf{p}'')\,[E(\mathbf{p}'')-E(\mathbf{p})]}\, Q_P[n_F(p'')]\,\mathcal{G}(\mathbf{p}'',\mathbf{p};W). \tag{A3}$$

This integral equation for the G-matrix is similar to that in the Dirac-Bruckner theory, see *e.g.* [64, 65]. Notice that in the non-relativistic limit $M/E = 1$ and Eqn. (A3) corresponds to the usual employed G-matrix equation in the many-body problem. In fact, the difference with Eqn. (1) of Refs. [66, 67] is largely a factor $(M/E(p''))^2$ under the integral, and the use of an effective density dependent mass in the Dirac spinors. Therefore, the momentum space evaluation of the G-matrix partial waves is wel known.

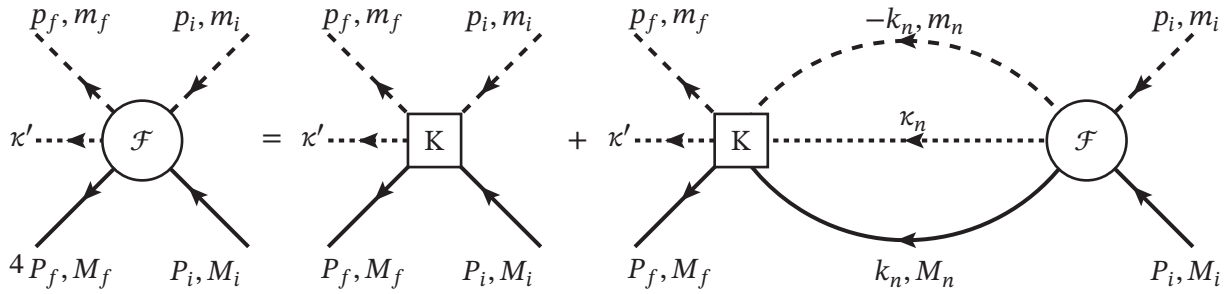

FIG. 7: G-matrix: Kadyshevsky-Bethe-Goldstone Equation

For a quark pair with flavor quantum numbers f_1, f_2 in quark matter the G-matrix equation for partial waves in short notation reads

$$G_{cc_0}(\omega) \;=\; K_{cc_0} + \sum_{c'} \left[\frac{m_Q}{(\epsilon_{f_1'} + \epsilon_{f_2'})}\right]^2 K_{cc'}\; \frac{Q_{y'}}{\omega - \epsilon_{f_1'} - \epsilon_{f_2'}}\; G_{c'c_0}(\omega), \tag{A4}$$

where c denotes the 'relative' state (y, T, L, S, J) with $y = (f_1, f_2)$. S and T are spin and isospin quantum numbers, respectively. The energies are $\epsilon_{f_i} = \sqrt{k_{f_i}^2 + m_Q^2} - m_Q$, i=1,2. The quark single particle (s.p.) energy ϵ_f in quark matter is

$$\epsilon_f(k_f) = \left[\sqrt{k_f^2 + m_Q^2}] - m_Q\right] + U_f(k_f), \tag{A5}$$

where k_f is the f-quark momentum ($\hbar = c = 1$). The potential energy U_f is (ontained self-consistently) in terms of the G-matrix as

$$U_f(k_f) \;=\; \sum_{|\mathbf{k}_{f'}|} \langle \mathbf{k}_f \mathbf{k}_{f'} | G_{ff'}\left(\omega = \epsilon_f(k_f) + \epsilon_{f'}(k_{f'}\right) | \mathbf{k}_f \mathbf{k}_{f'} \rangle. \tag{A6}$$

The kinetic, potential, and total energies per quark are given by averaged quantities of T_f, U_f, and $E_f = T_f + U_f$ in a Fermi sphere.

Appendix B: BBM-couplings in the QPC-model

The BBM-couplings in the ESC models fit very well with the ${}^3P_0 \oplus {}^3S_1$ quark-pair creation (QPC) model. A simple (effective) QPC interaction Lagrangian is

$$\mathcal{L}_I = \gamma \left[A \left(\sum_j \bar{q}_j\, q_j\right) \cdot \left(\sum_i \bar{q}_i\, q_i\right) + B \left(\sum_j \bar{q}_j \gamma_\mu\, q_j\right) \cdot \left(\sum_i \bar{q}_i \gamma^\mu\, q_i\right)\right], \tag{B1}$$

where γ, A, and B are given in Ref. [9] Table II. To see the meson couplings we make the Fierz transformation of (B1) which gives [68]

$$\begin{aligned} \mathcal{L}_I \;=\; -\frac{\gamma}{4} \sum_{i,j} \Big[& (A+4B)\bar{q}_i\, q_j \cdot \bar{q}_j\, q_i + (A-4B)\bar{q}_i \gamma_5 q_j \cdot \bar{q}_j \gamma^5 q_i \\ & + (A-2B)\bar{q}_i \gamma_\mu q_j \cdot \bar{q}_j \gamma^\mu q_i - (A+B)\bar{q}_i \gamma_\mu \gamma_5 q_j \cdot \bar{q}_j \gamma^\mu \gamma^5 q_i \\ & - (A/2)\, \bar{q}_i \sigma_{\mu\nu} q_j \cdot \bar{q}_j \sigma^{\mu\nu} q_i \Big]. \end{aligned} \tag{B2}$$

Identifying the $\bar{q}q$ pairs with the mesons

$$\chi^S_{ij} \;\sim\; \bar{q}_j\, q_i\;,\; \chi^P_{ij} \sim \bar{q}_j \gamma_5\, q_i\;,\; \chi^V_{\mu,ij} \sim \bar{q}_j \gamma_\mu q_i\;,\; \chi^A_{\mu,ij} \sim \bar{q}_j \gamma_5 \gamma_\mu q_i \tag{B3}$$

the QQM-couplings are defined. For example, the pseudoscalar couplings are

$$\mathcal{H}_P = g_8^{(p)} \sqrt{2} \left[\bar{Q} M_P^{(8)} Q\right] + g_1^{(p)} \left[\bar{Q} M_P^{(1)} Q\right] / \sqrt{3}, \tag{B4}$$

where $g_8^{(p)} = -\gamma_P (A - 4B)/4$.

Appendix C: Momentum-space Meson-Quark-Quark Vertices

1. Pauli-reduction Dirac-spinor Γ-matrix elements

The transition from Dirac spinors to Pauli spinors is given here, without approximations. We use the notations $\mathcal{E} = E + M$ and $\mathcal{E}' = E' + M'$, where $E = E(p, M)$ and $E' = E(p', M')$. Also, we omit, on the right-hand side in the expressions below, the final and initial Pauli spinors $\chi'^{\dagger}$ and χ respectively, which are self-evident.

$$\bar{u}(\mathbf{p}')u(\mathbf{p}) = +\sqrt{\frac{\mathcal{E}'\mathcal{E}}{4M'M}}\left[\left(1 - \frac{\mathbf{p}'\cdot\mathbf{p}}{\mathcal{E}'\mathcal{E}}\right) - i\frac{\mathbf{p}'\times\mathbf{p}\cdot\boldsymbol{\sigma}}{\mathcal{E}'\mathcal{E}}\right], \tag{C1a}$$

$$\bar{u}(\mathbf{p}')\gamma_5 u(\mathbf{p}) = -\sqrt{\frac{\mathcal{E}'\mathcal{E}}{4M'M}}\left[\frac{\boldsymbol{\sigma}\cdot\mathbf{p}'}{\mathcal{E}'} - \frac{\boldsymbol{\sigma}\cdot\mathbf{p}}{\mathcal{E}}\right], \tag{C1b}$$

$$\bar{u}(\mathbf{p}')\gamma^0 u(\mathbf{p}) = +\sqrt{\frac{\mathcal{E}'\mathcal{E}}{4M'M}}\left[\left(1 + \frac{\mathbf{p}'\cdot\mathbf{p}}{\mathcal{E}'\mathcal{E}}\right) + i\frac{\mathbf{p}'\times\mathbf{p}\cdot\boldsymbol{\sigma}}{\mathcal{E}'\mathcal{E}}\right], \tag{C1c}$$

$$\bar{u}(\mathbf{p}')\boldsymbol{\gamma}\, u(\mathbf{p}) = +\sqrt{\frac{\mathcal{E}'\mathcal{E}}{4M'M}}\left[\left(\frac{\mathbf{p}'}{\mathcal{E}'} + \frac{\mathbf{p}}{\mathcal{E}}\right) + i\left(\frac{\boldsymbol{\sigma}\times\mathbf{p}'}{\mathcal{E}'} - \frac{\boldsymbol{\sigma}\times\mathbf{p}}{\mathcal{E}}\right)\right], \tag{C1d}$$

$$\bar{u}(\mathbf{p}')\gamma_5\gamma^0 u(\mathbf{p}) = -\sqrt{\frac{\mathcal{E}'\mathcal{E}}{4M'M}}\left[\frac{\boldsymbol{\sigma}\cdot(\mathbf{p}'}{\mathcal{E}'} + \frac{\boldsymbol{\sigma}\cdot(\mathbf{p}}{\mathcal{E}}\right], \tag{C1e}$$

$$\begin{aligned}\bar{u}(\mathbf{p}')\gamma_5\boldsymbol{\gamma}\, u(\mathbf{p}) &= -\sqrt{\frac{\mathcal{E}'\mathcal{E}}{4M'M}}\left[\boldsymbol{\sigma} + \frac{(\boldsymbol{\sigma}\cdot\mathbf{p}')\,\boldsymbol{\sigma}\,(\boldsymbol{\sigma}\cdot\mathbf{p})}{\mathcal{E}'\mathcal{E}}\right] \\ &= -\sqrt{\frac{\mathcal{E}'\mathcal{E}}{4M'M}}\left[\left(1 - \frac{\mathbf{p}'\cdot\mathbf{p}}{\mathcal{E}'\mathcal{E}}\right)\boldsymbol{\sigma} - i\frac{\mathbf{p}'\times\mathbf{p}}{\mathcal{E}'\mathcal{E}}\right. \\ &\quad \left. + \frac{1}{\mathcal{E}'\mathcal{E}}\left(\boldsymbol{\sigma}\cdot\mathbf{p}\,\mathbf{p}' + \boldsymbol{\sigma}\cdot\mathbf{p}'\,\mathbf{p}\right)\right] \approx -\boldsymbol{\sigma},,\end{aligned} \tag{C1f}$$

where we defined $\mathbf{k} = \mathbf{p}' - \mathbf{p}$, $\mathbf{q} = (\mathbf{p}' + \mathbf{p})/2$, and $\kappa_V = f_V/g_V$.

Using the the Gordon decomposition

$$i\,\bar{u}(p')\,\sigma^{\mu\nu}(p' - p)_\nu u(p) = \bar{u}(p')\Big\{(M' + M)\gamma^\mu - (p' + p)^\mu\Big\}\,u(p) \tag{C2}$$

one obtains for the complete vector-vertex

$$\begin{aligned}
\bar{u}(p')\Gamma_V^\mu u(p) &\equiv \bar{u}(p')\left[\gamma^\mu + \frac{i}{2\mathcal{M}}\kappa_V\sigma^{\mu\nu}(p'-p)_\nu\right]u(p) \\
&= \bar{u}(p')\left[\left(1+\frac{M'+M}{2\mathcal{M}}\kappa_V\right)\gamma^\mu - \frac{\kappa_V}{2\mathcal{M}}(p'+p)_\mu\right]u(p) \Longrightarrow \\
\mu=0 \;:\; &+\sqrt{\frac{\mathcal{E}'\mathcal{E}}{4M'M}}\left[\left(1+\frac{M'+M}{2\mathcal{M}}\kappa_V\right)\left(1+\frac{\boldsymbol{\sigma}\cdot\mathbf{p}'\,\boldsymbol{\sigma}\cdot\mathbf{p}}{\mathcal{E}'\mathcal{E}}\right)\right. \\
&\left.-\frac{\kappa_V}{2\mathcal{M}}(E'+E)\left(1-\frac{\boldsymbol{\sigma}\cdot\mathbf{p}'\,\boldsymbol{\sigma}\cdot\mathbf{p}}{\mathcal{E}'\mathcal{E}}\right)\right], \qquad \text{(C3a)} \\
\mu=i \;:\; &+\sqrt{\frac{\mathcal{E}'\mathcal{E}}{4M'M}}\left[\left(1+\frac{M'+M}{2\mathcal{M}}\kappa_V\right)\left\{\left(\frac{\mathbf{p}'}{\mathcal{E}'}+\frac{\mathbf{p}}{\mathcal{E}}\right)+i\left(\frac{\boldsymbol{\sigma}\times\mathbf{p}'}{\mathcal{E}'}-\frac{\boldsymbol{\sigma}\times\mathbf{p}}{\mathcal{E}}\right)\right\}\right. \\
&\left.-\frac{\kappa_V}{2\mathcal{M}}(\mathbf{p}'+\mathbf{p})\left(1-\frac{\boldsymbol{\sigma}\cdot\mathbf{p}'\,\boldsymbol{\sigma}\cdot\mathbf{p}}{\mathcal{E}'\mathcal{E}}\right)\right]. \qquad \text{(C3b)}
\end{aligned}$$

2. 1/M-expansion Γ-matrix elements

The exact transition from Dirac spinors to Pauli spinors is given in Appendix C 1. From the expressions in C 1, keeping only terms up to order $1/M$, and setting the scaling mass $\mathcal{M} = M$, we find that the vertex operators in Pauli-spinor space for the NNm vertices are given by

$$\begin{aligned}
\bar{u}(\mathbf{p}')u(\mathbf{p}) &= \left[\left(1-\frac{\mathbf{p}'\cdot\mathbf{p}}{4M^2}\right)-\frac{i}{4M^2}\mathbf{p}'\times\mathbf{p}\cdot\boldsymbol{\sigma}\right], &\text{(C4a)}\\
\bar{u}(\mathbf{p}')\gamma_5 u(\mathbf{p}) &= -\frac{1}{2M}\big[\boldsymbol{\sigma}\cdot(\mathbf{p}'-\mathbf{p})\big] = -\frac{1}{2M}[\boldsymbol{\sigma}\cdot\mathbf{k}], &\text{(C4b)}\\
\bar{u}(\mathbf{p}')\gamma^0 u(\mathbf{p}) &= \left[\left(1+\frac{\mathbf{p}'\cdot\mathbf{p}}{4M^2}\right)+\frac{i}{4M^2}\mathbf{p}'\times\mathbf{p}\cdot\boldsymbol{\sigma}\right], &\text{(C4c)}\\
\bar{u}(\mathbf{p}')\boldsymbol{\gamma}\, u(\mathbf{p}) &= \frac{1}{2M}\big[(\mathbf{p}'+\mathbf{p})+i\boldsymbol{\sigma}\times(\mathbf{p}'-\mathbf{p})\big], &\text{(C4d)}\\
\bar{u}(\mathbf{p}')\gamma_5\gamma^0 u(\mathbf{p}) &= -\frac{1}{2M}\big[\boldsymbol{\sigma}\cdot(\mathbf{p}'+\mathbf{p})\big] = -\frac{1}{M}[\boldsymbol{\sigma}\cdot\mathbf{q}], &\text{(C4e)}\\
\bar{u}(\mathbf{p}')\gamma_5\boldsymbol{\gamma}\, u(\mathbf{p}) &= -\left[\boldsymbol{\sigma}+\frac{1}{4M^2}(\boldsymbol{\sigma}\cdot\mathbf{p}')\,\boldsymbol{\sigma}\,(\boldsymbol{\sigma}\cdot\mathbf{p})\right] = -\left[\left(1-\frac{\mathbf{p}'\cdot\mathbf{p}}{4M^2}\right)\boldsymbol{\sigma}\right. \\
&\left.-\frac{i}{4M^2}\mathbf{p}'\times\mathbf{p}+\frac{1}{4M^2}\left(\boldsymbol{\sigma}\cdot\mathbf{p}\,\mathbf{p}'+\boldsymbol{\sigma}\cdot\mathbf{p}'\,\mathbf{p}\right)\right] \approx -\boldsymbol{\sigma},, &\text{(C4f)}
\end{aligned}$$

where we defined $\mathbf{k} = \mathbf{p}' - \mathbf{p}$, $\mathbf{q} = (\mathbf{p}' + \mathbf{p})/2$, and $\kappa_V = f_V/g_V$. In passing we note that the inclusion of the $1/M^2$-terms is necessary in order to get spin-orbit potentials, like in the case of the OBE-potentials.

For the magnetic-coupling we use the Gordon decomposition

$$i\,\bar{u}(p')\,\sigma^{\mu\nu}(p'-p)_\nu u(p) = \bar{u}(p')\Big\{2M\gamma^\mu - (p'+p)^\mu\Big\}\,u(p) \qquad \text{(C5)}$$

We get

$$i\,\bar{u}(p')\,\sigma^{\mu\nu}(p'-p)_\nu u(p) \Longrightarrow$$

$$\mu=0\ :\ -M\left[\left(1-\frac{\mathbf{p}'\cdot\mathbf{p}}{4M^2}\right)+\frac{(p'^2+p^2)}{2M^2}-\frac{i}{4M^2}\mathbf{p}'\times\mathbf{p}\cdot\boldsymbol{\sigma}\right], \tag{C6a}$$

$$\mu=i\ :\ -\left[\frac{1}{2}(\mathbf{p}'+\mathbf{p})-\frac{i}{2}\boldsymbol{\sigma}\times(\mathbf{p}'-\mathbf{p})\right]. \tag{C6b}$$

For the vector-vertex with direct and derivative coupling one has

$$\begin{aligned}\bar{u}(p')\Gamma_V^\mu u(p) &\equiv \bar{u}(p')\left[\gamma^\mu+\frac{i}{2M}\kappa_V\sigma^{\mu\nu}(p'-p)_\nu\right]u(p)\\ &= \bar{u}(p')\left[(1+\kappa_V)\gamma^\mu-\frac{\kappa_V}{2M}(p'+p)_\mu\right]u(p)\Longrightarrow\end{aligned}$$

$$\begin{aligned}\mu=0\ :\ &\left[(1+\kappa_V)\left(1+\frac{\mathbf{p}'\cdot\mathbf{p}}{4M^2}+\frac{i}{4M^2}\mathbf{p}'\times\mathbf{p}\cdot\boldsymbol{\sigma}\right)\right.\\ &\left.-\kappa_V\frac{E_{p'}+E_p}{2M}\left(1-\frac{\mathbf{p}'\cdot\mathbf{p}}{4M^2}-\frac{i}{4M^2}\mathbf{p}'\times\mathbf{p}\cdot\boldsymbol{\sigma}\right)\right]\approx\\ &\left[1+(1+2\kappa_V)\left\{\frac{\mathbf{p}'\cdot\mathbf{p}}{4M^2}+\frac{i}{4M^2}\mathbf{p}'\times\mathbf{p}\cdot\boldsymbol{\sigma}\right\}-\kappa_V\frac{\mathbf{p}'^2+\mathbf{p}^2}{4M^2}\right],\end{aligned} \tag{C7a}$$

$$\mu=i\ :\ \frac{1}{M}\left[\frac{1}{2}(\mathbf{p}'+\mathbf{p})+\frac{i}{2}(1+\kappa_V)\boldsymbol{\sigma}\times(\mathbf{p}'-\mathbf{p})\right]. \tag{C7b}$$

3. Complete Meson-vertices in Pauli-spinor space

The transition from Dirac spinors to Pauli spinors is reviewed in Appendix C of [37]. Following this reference and keeping only terms up to order $(1/M)^2$, we find that the vertex operators in Pauli-spinor space for the QQm vertices are given by

$$\bar{u}(\mathbf{p}')\Gamma_P^{(1)}u(\mathbf{p}) = -i\frac{f_P}{m_\pi}\left[\boldsymbol{\sigma}_1\cdot\mathbf{k}\pm\frac{\omega}{2M}\boldsymbol{\sigma}_1\cdot(\mathbf{p}'+\mathbf{p})\right], \tag{C8a}$$

$$\begin{aligned}\bar{u}(\mathbf{p}')\Gamma_V^{(1)}u(\mathbf{p}) = g_V\left[\left\{\left(1+\frac{\mathbf{p}'\cdot\mathbf{p}}{4M^2}\right)-\frac{i}{4M^2}\mathbf{p}'\times\mathbf{p}\cdot\boldsymbol{\sigma}\right\}\phi_V^0\right.\\ \left.-\frac{1}{2M}\left\{(\mathbf{p}'+\mathbf{p})+i(1+\kappa_V)\boldsymbol{\sigma}_1\times\mathbf{k}\right\}\cdot\boldsymbol{\phi}_V\right],\end{aligned} \tag{C8b}$$

$$\begin{aligned}\bar{u}(\mathbf{p}')\Gamma_A^{(1)}u(\mathbf{p}) = g_A\left[-\frac{1}{2M}\left\{\boldsymbol{\sigma}\cdot(\mathbf{p}'+\mathbf{p})\right\}\phi_A^0\right.\\ \left.+\left\{\boldsymbol{\sigma}+\frac{1}{4M^2}(\boldsymbol{\sigma}\cdot\mathbf{p}')\,\boldsymbol{\sigma}\,(\boldsymbol{\sigma}\cdot\mathbf{p})\right\}\cdot\boldsymbol{\phi}_A\right],\end{aligned} \tag{C8c}$$

$$\bar{u}(\mathbf{p}')\Gamma_S^{(1)}u(\mathbf{p}) = g_S\left[\left(1-\frac{\mathbf{p}'\cdot\mathbf{p}}{4M^2}\right)-\frac{i}{4M^2}\mathbf{p}'\times\mathbf{p}\cdot\boldsymbol{\sigma}\right], \tag{C8d}$$

where we defined $\mathbf{k}=\mathbf{p}'-\mathbf{p}$ and $\kappa_V=f_V/g_V$. In the pseudovector vertex, the upper (lower) sign stands for creation (absorption) of the pion at the vertex. In passing we note that the inclusion of the

$1/M^2$-terms is necessary in order to get spin-orbit potentials, like in the case of the OBE-potentials.

The complete quark-meson verices are:
(i) Scalar mesons: Including the extra quark-level coupling

$$\bar{u}(\mathbf{p}')\Gamma_S u(\mathbf{p}) \;=\; g_S\left(1-\frac{\mathbf{k}^2}{4m_Q^2}\right)\left[\left(1-\frac{\mathbf{p}'\cdot\mathbf{p}}{4M^2}\right)-\frac{i}{4M^2}\mathbf{p}'\times\mathbf{p}\cdot\boldsymbol{\sigma}\right], \tag{C9}$$

(ii) Vector mesons: For the complete vector-meson coupling to the quarks

$$\Gamma_V^\mu = G_m\gamma^\mu+\frac{1}{\mathcal{M}}G_e(p'+p)^\mu,\; G_{m,v}=g_v+f_v\;,\; G_{e,v}=-f_v\left[1+\frac{k^2}{8m_Q^2}\right],$$

and writing $\Gamma_V=\Gamma_V^{(m)}+\Gamma_V^{(e)}$,

$$\begin{aligned}
\bar{u}(\mathbf{p}')\Gamma_V^{(m)}u(\mathbf{p}) \;&=\; G_{m,v}\left[\left\{\left(1+\frac{\mathbf{p}'\cdot\mathbf{p}}{4M^2}\right)+\frac{i}{4M^2}\mathbf{p}'\times\mathbf{p}\cdot\boldsymbol{\sigma}\right\}\phi_V^0\right.\\
&\qquad\left.+\frac{1}{2M}\left\{(\mathbf{p}'+\mathbf{p})+i\boldsymbol{\sigma}_1\times\mathbf{k}\right\}\cdot\boldsymbol{\phi}_V\right], \qquad\text{(C10a)}\\
\bar{u}(\mathbf{p}')\Gamma_V^{(e)}u(\mathbf{p}) \;&=\; G_{e,v}\left[\frac{\mathcal{E}'+\mathcal{E}}{\mathcal{M}}\left\{\left(1-\frac{\mathbf{p}'\cdot\mathbf{p}}{4M^2}\right)-\frac{i}{4M^2}\mathbf{p}'\times\mathbf{p}\cdot\boldsymbol{\sigma}\right\}\phi_V^0\right.\\
&\qquad\left.+\frac{(\mathbf{p}'+\mathbf{p})}{\mathcal{M}}\left\{\left(1-\frac{\mathbf{p}'\cdot\mathbf{p}}{4M^2}\right)-\frac{i}{4M^2}\mathbf{p}'\times\mathbf{p}\cdot\boldsymbol{\sigma}\right\}\right]\cdot\boldsymbol{\phi}_V\\
&\approx\; G_{e,v}\left[2\frac{M}{\mathcal{M}}\left\{\left(1+\frac{\mathbf{p}'^2-\mathbf{p}'\cdot\mathbf{p}+\mathbf{p}^2}{4M^2}\right)-\frac{i}{4M^2}\mathbf{p}'\times\mathbf{p}\cdot\boldsymbol{\sigma}\right\}\phi_V^0+\frac{(\mathbf{p}'+\mathbf{p})}{\mathcal{M}}\right\}\cdot\boldsymbol{\phi}_V\Big] \qquad\text{(C10b)}
\end{aligned}$$

(iii) Axial-vector mesons: The extra QQ axial-coupling has the vertex

$$\begin{aligned}
\bar{u}(\mathbf{p}')\Gamma_A^{(o)}u(\mathbf{p}) \;&=\; \frac{g_a'}{\mathcal{M}^2}\left[\frac{1}{M}\left\{(\mathbf{p}'\cdot\mathbf{p}-\mathbf{p}^2)\boldsymbol{\sigma}\cdot\mathbf{p}'+(\mathbf{p}'\cdot\mathbf{p}-\mathbf{p}'^2)\boldsymbol{\sigma}\cdot\mathbf{p}\right\}\phi_A^0-2i\mathbf{p}'\times\mathbf{p}\cdot\boldsymbol{\phi}_A\right]\\
&=\; \frac{g_a}{4\mathcal{M}^2}\left[\frac{1}{M}\left\{(\mathbf{q}\cdot\mathbf{k}\,\boldsymbol{\sigma}\cdot\mathbf{k}-\mathbf{k}^2\,\boldsymbol{\sigma}\cdot\mathbf{q}\right\}\phi_A^0+2i\mathbf{q}\times\mathbf{k}\cdot\boldsymbol{\phi}_A\right]\\
&\approx\; \frac{g_a}{2\mathcal{M}^2}\cdot i\mathbf{q}\times\mathbf{k}\cdot\boldsymbol{\phi}_A, \qquad\text{(C11)}
\end{aligned}$$

i.e. a purely spin-orbit contribution. Using

$$\begin{aligned}
&(\boldsymbol{\sigma}\cdot\mathbf{p}')\,\boldsymbol{\sigma}\,(\boldsymbol{\sigma}\cdot\mathbf{p})=\mathbf{p}'\,(\boldsymbol{\sigma}\cdot\mathbf{p})+\mathbf{p}\,(\boldsymbol{\sigma}\cdot\mathbf{p}')-\mathbf{p}'\cdot\mathbf{p}\,\boldsymbol{\sigma}-i\mathbf{p}'\times\mathbf{p}=\\
&2\mathbf{q}(\boldsymbol{\sigma}\cdot\mathbf{q})-\frac{1}{2}\mathbf{k}\,(\boldsymbol{\sigma}\cdot\mathbf{k})-(\mathbf{q}^2-\mathbf{k}^2/4)\,\boldsymbol{\sigma}+i\mathbf{q}\times\mathbf{k}.\div
\end{aligned}$$

we obtain for the complete axial-vertex, with $\mathcal{M}=M$,

$$\begin{aligned}
\bar{u}(\mathbf{p}')\Gamma_A u(\mathbf{p}) \;&=\; g_A\left[-\frac{1}{M}(\boldsymbol{\sigma}\cdot\mathbf{q})\phi_A^0+\left\{\boldsymbol{\sigma}\left(1-\frac{\mathbf{q}^2-\mathbf{k}^2/4}{4M^2}\right)\right.\right.\\
&\qquad\left.\left.+\frac{1}{4M^2}\left(2\mathbf{q}(\boldsymbol{\sigma}\cdot\mathbf{q})-\frac{1}{2}\mathbf{k}(\boldsymbol{\sigma}\cdot\mathbf{k})\right)+\frac{3i}{4M^2}\mathbf{q}\times\mathbf{k}\right\}\cdot\boldsymbol{\phi}_A\right]. \qquad\text{(C12)}
\end{aligned}$$

Appendix D: One-Boson-Exchange Quark-quark Potentials

1. Non-strange Meson-exchange

For the non-strange mesons the mass differences at the vertices are neglected, we take at the QQM- and NNM-vertex the average quark and average nucleon mass respectively. This implies that we do not include contributions to the Pauli-invariants P_7 and P_8. For vector-, and diffractive OBE-exchange we refer the reader to Ref. [40], where the contributions to the different $\Omega_i^{(X)}$'s for baryon-baryon scattering are given in detail.
Below, for QQ: $M_n = M_y = M_Q$, and for QN: $M_y = M_Q, M_n = M_N$. For QQ-channels: $g^x_{13} = (g^x_{QQ})_{13}$ and $g^x_{24} = (g^x_{QQ})_{24}$ etc., and for QN-channels $g^x_{13} = (g^x_{QQ})_{13}$ and $g^x_{24} = (g^x_{NN})_{24}$ etc., where x=p,pv,v,a, and b.

(a) Pseudoscalar-meson exchange:

$$\Omega^{(P)}_{2a} = -g^p_{13}g^p_{24}\left(\frac{\mathbf{k}^2}{12M_yM_n}\right) \ , \ \Omega^{(P)}_{3a} = -g^p_{13}g^p_{24}\left(\frac{1}{4M_yM_n}\right), \tag{D1a}$$

$$\Omega^{(P)}_{2b} = +g^p_{13}g^p_{24}\left(\frac{\mathbf{k}^2}{24M_y^2M_n^2}\right) \ , \ \Omega^{(P)}_{3b} = +g^p_{13}g^p_{24}\left(\frac{1}{8M_y^2M_n^2}\right),. \tag{D1b}$$

PV-formulas:

$$\Omega^{(P)}_{2a} = -f^{pv}_{13}f^{pv}_{24}\left(\frac{\mathbf{k}^2}{3m^2_{\pi^+}}\right) \ , \ \Omega^{(P)}_{3a} = -f^{pv}_{13}f^{pv}_{24}\left(\frac{1}{m^2_{\pi^+}}\right), \tag{D1c}$$

$$\Omega^{(P)}_{2b} = +f^{pv}_{13}f^{pv}_{24}\left(\frac{\mathbf{k}^2}{6m^2_{\pi^+}M_yM_n}\right) \ , \ \Omega^{(P)}_{3b} = +f^{pv}_{13}f^{pv}_{24}\left(\frac{1}{2m^2_{\pi^+}M_y^2M_n^2}\right),. \tag{D1d}$$

(b) Vector-meson exchange:

$$\begin{aligned}
\Omega^{(V)}_{1a} &= \left\{g^v_{13}g^v_{24}\left(1-\frac{\mathbf{k}^2}{2M_yM_n}\right) - g^v_{13}f^v_{24}\frac{\mathbf{k}^2}{4\mathcal{M}M_n} - f^v_{13}g^v_{24}\frac{\mathbf{k}^2}{4\mathcal{M}M_y}\right. \\
&\quad \left. + f^v_{13}f^v_{24}\frac{\mathbf{k}^4}{16\mathcal{M}^2M_yM_n}\right\}, \ \Omega^{(V)}_{1b} = g^v_{13}g^v_{24}\left(\frac{3}{2M_yM_n}\right), \\
\Omega^{(V)}_{2a} &= -\frac{2}{3}\mathbf{k}^2\,\Omega^{(V)}_{3a}, \ \Omega^{(V)}_{2b} = -\frac{2}{3}\mathbf{k}^2\,\Omega^{(V)}_{3b}, \\
\Omega^{(V)}_{3a} &= \left\{(g^v_{13}+f^v_{13}\frac{M_y}{\mathcal{M}})(g^v_{24}+f^v_{24}\frac{M_n}{\mathcal{M}}) - f^v_{13}f^v_{24}\frac{\mathbf{k}^2}{8\mathcal{M}^2}\right\}/(4M_yM_n), \\
\Omega^{(V)}_{3b} &= -(g^v_{13}+f^v_{13}\frac{M_y}{\mathcal{M}})(g^v_{24}+f^v_{24}\frac{M_n}{\mathcal{M}})/(8M_y^2M_n^2), \\
\Omega^{(V)}_{4} &= -\left\{12g^v_{13}g^v_{24} + 8(g^v_{13}f^v_{24}+f^v_{13}g^v_{24})\frac{\sqrt{M_yM_n}}{\mathcal{M}} - f^v_{13}f^v_{24}\frac{3\mathbf{k}^2}{\mathcal{M}^2}\right\}/(8M_yM_n) \\
\Omega^{(V)}_{5} &= -\left\{g^v_{13}g^v_{24} + 4(g^v_{13}f^v_{24}+f^v_{13}g^v_{24})\frac{\sqrt{M_yM_n}}{\mathcal{M}} + 8f^v_{13}f^v_{24}\frac{M_yM_n}{\mathcal{M}^2}\right\}/(16M_y^2M_n^2) \\
\Omega^{(V)}_{6} &= -\left\{(g^v_{13}g^v_{24}+f^v_{13}f^v_{24}\frac{\mathbf{k}^2}{4\mathcal{M}^2})\frac{(M_n^2-M_y^2)}{4M_y^2M_n^2} - (g^v_{13}f^v_{24}-f^v_{13}g^v_{24})\frac{1}{\sqrt{\mathcal{M}^2M_yM_n}}\right\}.
\end{aligned} \tag{D2}$$

(c) Scalar-meson exchange:

$$\begin{aligned}
\Omega_{1a}^{(S)} &= -g_{13}^s g_{24}^s \left(1+\frac{\mathbf{k}^2}{4M_yM_n}\right) \\
\Omega_{1b}^{(S)} &= +g_{13}^s g_{24}^s \left[\frac{1}{2M_yM_n}\right] \;,\; \Omega_4^{(S)} = -g_{13}^s g_{24}^s \left[\frac{1}{2M_yM_n}\right] \\
\Omega_5^{(S)} &= g_{13}^s g_{24}^s \left[\frac{1}{16M_y^2M_n^2}\right] \;,\; \Omega_6^{(S)} = -g_{13}^s g_{24}^s \frac{(M_n^2-M_y^2)}{4M_y^2M_n^2}.
\end{aligned} \tag{D3}$$

(d) Axial-vector-exchange $J^{PC}=1^{++}$:

$$\begin{aligned}
\Omega_{2a}^{(A)} &= -g_{13}^a g_{24}^a \left[1-\frac{2\mathbf{k}^2}{3M_yM_n}\right] + \left[\left(g_{13}^A f_{24}^A \frac{M_n}{\mathcal{M}} + f_{13}^A g_{24}^A \frac{M_y}{\mathcal{M}}\right) - f_{13}^A f_{24}^A \frac{\mathbf{k}^2}{2\mathcal{M}^2}\right] \frac{\mathbf{k}^2}{6M_yM_n} \\
\Omega_{2b}^{(A)} &= -g_{13}^a g_{24}^a \left(\frac{3}{2M_yM_n}\right) \\
\Omega_3^{(A)} &= -g_{13}^a g_{24}^a \left[\frac{1}{4M_yM_n}\right] + \left[\left(g_{13}^A f_{24}^A \frac{M_n}{\mathcal{M}} + f_{13}^A g_{24}^A \frac{M_y}{\mathcal{M}}\right) - f_{13}^A f_{24}^A \frac{\mathbf{k}^2}{2\mathcal{M}^2}\right] \frac{1}{2M_yM_n} \\
\Omega_4^{(A)} &= -g_{13}^a g_{24}^a \left[\frac{1}{2M_yM_n}\right] \;,\; \Omega_6^{(A)} = -g_{13}^a g_{24}^a \left[\frac{(M_n^2-M_y^2)}{4M_y^2M_n^2}\right] \\
\Omega_5^{(A)'} &= -g_{13}^a g_{24}^a \left[\frac{2}{M_yM_n}\right]
\end{aligned} \tag{D4}$$

Here, we used the B-field description with $\alpha_r = 1$, see [13] Appendix A. The detailed treatment of the potential proportional to P_5', i.e. with $\Omega_5^{(A)'}$, is given in [13], Appendix B.

(e) Axial-vector mesons with $J^{PC}=1^{+-}$:

$$\begin{aligned}
\Omega_{2a}^{(B)} &= +f_{13}^B f_{24}^B \frac{(M_n+M_y)^2}{m_B^2}\left(1-\frac{\mathbf{k}^2}{4M_yM_n}\right)\left(\frac{\mathbf{k}^2}{12M_yM_n}\right),\; \Omega_{2b}^{(B)} = +f_{13}^B f_{24}^B \frac{(M_n+M_y)^2}{m_B^2}\left(\frac{\mathbf{k}^2}{8M_y^2M_n^2}\right) \\
\Omega_{3a}^{(B)} &= +f_{13}^B f_{24}^B \frac{(M_n+M_y)^2}{m_B^2}\left(1-\frac{\mathbf{k}^2}{4M_yM_n}\right)\left(\frac{1}{4M_yM_n}\right),\; \Omega_{3b}^{(B)} = +f_{13}^B f_{24}^B \frac{(M_n+M_y)^2}{m_B^2}\left(\frac{3}{8M_y^2M_n^2}\right).
\end{aligned} \tag{D5}$$

(f) Diffractive-exchange (pomeron, f, f', A_2):
The Ω_i^D are the same as for scalar-meson-exchange Eq.(D3), but with $\pm g_{13}^S g_{24}^S$ replaced by $\mp g_{13}^D g_{24}^D$, and except for the zero in the form factor.

(g) Odderon-exchange: The Ω_i^O are the same as for vector-meson-exchange Eq.(refeq2), but with $g_{13}^V \to g_{13}^O$, $f_{13}^V \to f_{13}^O$ and similarly for the couplings with the 24-subscript.

As in Ref. [40] in the derivation of the expressions for $\Omega_i^{(X)}$, given above, M_y and M_n denote the mean hyperon and nucleon mass, respectively $M_y = (M_1+M_3)/2$ and $M_n = (M_2+M_4)/2$, and m denotes the mass of the exchanged meson. Moreover, the approximation $1/M_N^2 + 1/M_Y^2 \approx 2/M_nM_y$, is used, which is rather good since the mass differences between the baryons are not large.

2. One-Boson-Exchange Interactions in Configuration Space I

In configuration space the BB-interactions are described by potentials of the general form

$$V = \Big\{V_C(r) + V_\sigma(r)\boldsymbol{\sigma}_1\cdot\boldsymbol{\sigma}_2 + V_T(r)S_{12} + V_{SO}(r)\mathbf{L}\cdot\mathbf{S} + V_Q(r)Q_{12} + V_{ASO}(r)\,\frac{1}{2}(\boldsymbol{\sigma}_1-\boldsymbol{\sigma}_2)\cdot\mathbf{L} - \frac{1}{2M_yM_n}\left(\boldsymbol{\nabla}^2V^{n.l.}(r) + V^{n.l.}(r)\boldsymbol{\nabla}^2\right)\Big\}\cdot\mathcal{P}, \tag{D6a}$$

$$V^{n.l.} = \Big\{\varphi_C(r) + \varphi_\sigma(r)\boldsymbol{\sigma}_1\cdot\boldsymbol{\sigma}_2 + \varphi_T(r)S_{12}\Big\}\cdot\mathcal{P}, \tag{D6b}$$

where for non-strange mesons $\mathcal{P}=1$, and

$$S_{12} = 3(\boldsymbol{\sigma}_1\cdot\hat{r})(\boldsymbol{\sigma}_2\cdot\hat{r}) - (\boldsymbol{\sigma}_1\cdot\boldsymbol{\sigma}_2), \tag{D7a}$$

$$Q_{12} = \frac{1}{2}\Big[(\boldsymbol{\sigma}_1\cdot\mathbf{L})(\boldsymbol{\sigma}_2\cdot\mathbf{L}) + (\boldsymbol{\sigma}_2\cdot\mathbf{L})(\boldsymbol{\sigma}_1\cdot\mathbf{L})\Big], \tag{D7b}$$

$$\phi(r) = \phi_C(r) + \phi_\sigma(r)\boldsymbol{\sigma}_1\cdot\boldsymbol{\sigma}_2, \tag{D7c}$$

For the basic functions for the Fourier transforms with gaussian form factors, we refer to Refs. [39, 40]. For the details of the Fourier transform for the potentials with P_5', which occur in the case of the axial-vector mesons with $J^{PC}=1^{++}$, we refer to Ref. [13] Appendix B.
(a) Pseudoscalar-meson-exchange:

$$V_{PS}(r) = \frac{m}{4\pi}\left[g_{13}^p g_{24}^p \frac{m^2}{4M_yM_n}\left(\frac{1}{3}(\boldsymbol{\sigma}_1\cdot\boldsymbol{\sigma}_2)\,\phi_C^1 + S_{12}\phi_T^0\right)\right]\mathcal{P}, \tag{D8a}$$

$$V_{PS}^{n.l.}(r) = \frac{m}{4\pi}\left[g_{13}^p g_{24}^p \frac{m^2}{4M_yM_n}\left(\frac{1}{3}(\boldsymbol{\sigma}_1\cdot\boldsymbol{\sigma}_2)\,\phi_C^1 + S_{12}\phi_T^0\right)\right]\mathcal{P}. \tag{D8b}$$

(b) Vector-meson-exchange:

$$
\begin{aligned}
V_V(r) = \frac{m}{4\pi}\Bigg[&\Bigg\{g_{13}^{v}g_{24}^{v}\left[\phi_C^0+\frac{m^2}{2M_yM_n}\phi_C^1\right]\\
&+\left[g_{13}^{v}f_{24}^{v}\frac{m^2}{4\mathcal{M}M_n}+f_{13}^{v}g_{24}^{v}\frac{m^2}{4\mathcal{M}M_y}\right]\phi_C^1+f_{13}^{v}f_{24}^{v}\frac{m^4}{16\mathcal{M}^2M_yM_n}\phi_C^2\Bigg\}\\
&+\frac{m^2}{6M_yM_n}\left\{\left[\left(g_{13}^{v}+f_{13}^{v}\frac{M_y}{\mathcal{M}}\right)\cdot\left(g_{24}^{v}+f_{24}^{v}\frac{M_n}{\mathcal{M}}\right)\right]\phi_C^1+f_{13}^{v}f_{24}^{v}\frac{m^2}{8\mathcal{M}^2}\phi_C^2\right\}(\boldsymbol{\sigma}_1\cdot\boldsymbol{\sigma}_2)\\
&-\frac{m^2}{4M_yM_n}\left\{\left[\left(g_{13}^{v}+f_{13}^{v}\frac{M_y}{\mathcal{M}}\right)\cdot\left(g_{24}^{v}+f_{24}^{v}\frac{M_n}{\mathcal{M}}\right)\right]\phi_T^0+f_{13}^{v}f_{24}^{v}\frac{m^2}{8\mathcal{M}^2}\phi_T^1\right\}S_{12}\\
&-\frac{m^2}{M_yM_n}\left\{\left[\frac{3}{2}g_{13}^{v}g_{24}^{v}+\left(g_{13}^{v}f_{24}^{v}+f_{13}^{v}g_{24}^{v}\right)\frac{\sqrt{M_yM_n}}{\mathcal{M}}\right]\phi_{SO}^0+\frac{3}{8}f_{13}^{v}f_{24}^{v}\frac{m^2}{\mathcal{M}^2}\phi_{SO}^1\right\}\mathbf{L}\cdot\mathbf{S}\\
&+\frac{m^4}{16M_y^2M_n^2}\left\{\left[g_{13}^{v}g_{24}^{v}+4\left(g_{13}^{v}f_{24}^{v}+f_{13}^{v}g_{24}^{v}\right)\frac{\sqrt{M_yM_n}}{\mathcal{M}}+8f_{13}^{v}f_{24}^{v}\frac{M_yM_n}{\mathcal{M}^2}\right]\right\}\cdot\\
&\times\frac{3}{(mr)^2}\phi_T^0Q_{12}-\frac{m^2}{M_yM_n}\Bigg\{\Bigg[\left(g_{13}^{v}g_{24}^{v}-f_{13}^{v}f_{24}^{v}\frac{m^2}{\mathcal{M}^2}\right)\frac{(M_n^2-M_y^2)}{4M_yM_n}\\
&-\left(g_{13}^{v}f_{24}^{v}-f_{13}^{v}g_{24}^{v}\right)\frac{\sqrt{M_yM_n}}{\mathcal{M}}\Bigg]\phi_{SO}^0\Bigg\}\cdot\frac{1}{2}(\boldsymbol{\sigma}_1-\boldsymbol{\sigma}_2)\cdot\mathbf{L}\Bigg]\mathcal{P},
\end{aligned}
\tag{D9a}
$$

$$
\begin{aligned}
V_V^{n.l.}(r) = \frac{m}{4\pi}\Bigg[&\frac{3}{2}g_{13}^{v}g_{24}^{v}\,\phi_C^0\\
&+\frac{m^2}{6M_yM_n}\left\{\left[\left(g_{13}^{v}+f_{13}^{v}\frac{M_y}{\mathcal{M}}\right)\cdot\left(g_{24}^{v}+f_{24}^{v}\frac{M_n}{\mathcal{M}}\right)\right]\phi_C^1\right\}(\boldsymbol{\sigma}_1\cdot\boldsymbol{\sigma}_2)\\
&-\frac{m^2}{4M_yM_n}\left\{\left[\left(g_{13}^{v}+f_{13}^{v}\frac{M_y}{\mathcal{M}}\right)\cdot\left(g_{24}^{v}+f_{24}^{v}\frac{M_n}{\mathcal{M}}\right)\right]\phi_T^0\right\}S_{12}\Bigg]\mathcal{P}.
\end{aligned}
\tag{D9b}
$$

Note: the non-local tensor and "associated" spin-spin terms are not included in ESC16 model.

(c) Scalar-meson-exchange:

$$
\begin{aligned}
V_S(r) \;=\; -\frac{m}{4\pi}\Bigg[&g_{13}^{s}g_{24}^{s}\Bigg\{\left[\phi_C^0-\frac{m^2}{4M_yM_n}\phi_C^1\right]+\frac{m^2}{2M_yM_n}\phi_{SO}^0\,\mathbf{L}\cdot\mathbf{S}+\frac{m^4}{16M_y^2M_n^2}\cdot\\
&\times\frac{3}{(mr)^2}\phi_T^0Q_{12}+\frac{m^2}{M_yM_n}\left[\frac{(M_n^2-M_y^2)}{4M_yM_n}\right]\phi_{SO}^0\cdot\frac{1}{2}(\boldsymbol{\sigma}_1-\boldsymbol{\sigma}_2)\cdot\mathbf{L}\\
&+\frac{1}{4M_yM_n}\left(\boldsymbol{\nabla}^2\phi_C^0+\phi_C^0\boldsymbol{\nabla}^2\right)\Bigg\}\Bigg]\mathcal{P}.
\end{aligned}
\tag{D10}
$$

(d) Axial-vector-meson exchange $J^{PC} = 1^{++}$:

$$
\begin{aligned}
V_A(r) = -\frac{m}{4\pi}\Bigg[&\Bigg\{g^a_{13}g^a_{24}\left(\phi^0_C + \frac{2m^2}{3M_yM_n}\phi^1_C\right) + \frac{m^2}{6M_yM_n}\left(g^a_{13}f^a_{24}\frac{M_n}{\mathcal{M}} + f^a_{13}g^a_{24}\frac{M_y}{\mathcal{M}}\right)\phi^1_C \\
&+ f^a_{13}f^a_{24}\frac{m^4}{12M_yM_n\mathcal{M}^2}\phi^2_C\Bigg\}(\boldsymbol{\sigma}_1\cdot\boldsymbol{\sigma}_2) - \frac{3}{4M_yM_n}g^a_{13}g^a_{24}\left(\boldsymbol{\nabla}^2\phi^0_C + \phi^0_C\boldsymbol{\nabla}^2\right)(\boldsymbol{\sigma}_1\cdot\boldsymbol{\sigma}_2) \\
&-\frac{m^2}{4M_yM_n}\Bigg\{\left[g^a_{13}g^a_{24} - 2\left(g^a_{13}f^a_{24}\frac{M_n}{\mathcal{M}} + f^a_{13}g^a_{24}\frac{M_y}{\mathcal{M}}\right)\right]\phi^0_T - f^a_{13}f^a_{24}\frac{m^2}{\mathcal{M}^2}\phi^1_T\Bigg\}S_{12} \\
&+\frac{m^2}{2M_yM_n}g^a_{13}g^a_{24}\left\{\phi^0_{SO}\,\mathbf{L}\cdot\mathbf{S} + \frac{m^2}{M_yM_n}\left[\frac{(M_n^2 - M_y^2)}{4M_yM_n}\right]\phi^0_{SO}\cdot\frac{1}{2}(\boldsymbol{\sigma}_1 - \boldsymbol{\sigma}_2)\cdot\mathbf{L}\right\}\Bigg]\mathcal{P}.
\end{aligned}
\tag{D11}
$$

(e) Axial-vector-meson exchange $J^{PC} = 1^{+-}$:

$$
\begin{aligned}
V_B(r) \;=\; &-\frac{m}{4\pi}\frac{(M_n + M_y)^2}{m^2}\Bigg[f^B_{13}f^B_{24}\Bigg\{\frac{m^2}{12M_yM_n}\left(\phi^1_C + \frac{m^2}{4M_yM_n}\phi^2_C\right)(\boldsymbol{\sigma}_1\cdot\boldsymbol{\sigma}_2) \\
&-\frac{m^2}{8M_yM_n}\left(\boldsymbol{\nabla}^2\phi^1_C + \phi^1_C\boldsymbol{\nabla}^2\right)(\boldsymbol{\sigma}_1\cdot\boldsymbol{\sigma}_2) + \left[\frac{m^2}{4M_yM_n}\right]\phi^0_T\,S_{12}\Bigg\}\Bigg]\mathcal{P},
\end{aligned}
\tag{D12a}
$$

$$
V^{n.l.}_B(r) \;=\; -\frac{m}{4\pi}\frac{(M_n + M_y)^2}{m^2}\left[f^B_{13}f^B_{24}\left\{\frac{3m^2}{4M_yM_n}\left(\frac{1}{3}\boldsymbol{\sigma}_1\cdot\boldsymbol{\sigma}_2\,\phi^1_C + S_{12}\,\phi^0_T\right)\right\}\right]\mathcal{P}.
\tag{D12b}
$$

(f) Diffractive exchange:

$$
\begin{aligned}
V_D(r) = \frac{m_P}{4\pi}\Bigg[&g^D_{13}g^D_{24}\frac{4}{\sqrt{\pi}}\frac{m_P^2}{\mathcal{M}^2}\cdot\Bigg[\Bigg\{1 + \frac{m_P^2}{2M_yM_n}(3 - 2m_P^2r^2) + \frac{m_P^2}{M_yM_n}\mathbf{L}\cdot\mathbf{S} \\
&+\left(\frac{m_P^2}{2M_yM_n}\right)^2 Q_{12} + \frac{m_P^2}{M_yM_n}\left[\frac{(M_n^2 - M_y^2)}{4M_yM_n}\right]\cdot\frac{1}{2}(\boldsymbol{\sigma}_1 - \boldsymbol{\sigma}_2)\cdot\mathbf{L}\Bigg\}\,e^{-m_P^2r^2} \\
&+\frac{1}{4M_yM_n}\left(\boldsymbol{\nabla}^2e^{-m_P^2r^2} + e^{-m_P^2r^2}\boldsymbol{\nabla}^2\right)\Bigg]\Bigg]\mathcal{P}.
\end{aligned}
\tag{D13}
$$

(g) Odderon-exchange:

$$V_{O,C}(r) = +\frac{g^O_{13}g^O_{24}}{4\pi}\frac{8}{\sqrt{\pi}}\frac{m_O^5}{\mathcal{M}^4}\left[(3-2m_O^2r^2)\right.$$
$$\left.-\frac{m_O^2}{M_yM_n}\left(15-20m_O^2r^2+4m_O^4r^4\right)\right]\exp(-m_O^2r^2)\,, \tag{D14a}$$

$$V_{O,n.l.}(r) = -\frac{g^O_{13}g^O_{24}}{4\pi}\frac{8}{\sqrt{\pi}}\frac{m_O^5}{\mathcal{M}^4}\frac{3}{4M_yM_n}\left\{\boldsymbol{\nabla}^2\left[(3-2m_O^2r^2)\exp(-m_O^2r^2)\right]+\right.$$
$$\left.+\left[(3-2m_O^2r^2)\exp(-m_O^2r^2)\right]\boldsymbol{\nabla}^2\right\}\,, \tag{D14b}$$

$$V_{O,\sigma}(r) = -\frac{g^O_{13}g^O_{24}}{4\pi}\frac{8}{3\sqrt{\pi}}\frac{m_O^5}{\mathcal{M}^4}\frac{m_O^2}{M_yM_n}\left[15-20m_O^2r^2+4m_O^4r^4\right]\exp(-m_O^2r^2)\cdot$$
$$\times\left(1+\kappa^O_{13}\frac{M_y}{\mathcal{M}}\right)\left(1+\kappa^O_{24}\frac{M_n}{\mathcal{M}}\right), \tag{D14c}$$

$$V_{O,T}(r) = -\frac{g^O_{13}g^O_{24}}{4\pi}\frac{8}{3\sqrt{\pi}}\frac{m_O^5}{\mathcal{M}^4}\frac{m_O^2}{M_yM_n}\cdot m_O^2r^2\left[7-2m_O^2r^2\right]\exp(-m_O^2r^2)\cdot$$
$$\times\left(1+\kappa^O_{13}\frac{M_y}{\mathcal{M}}\right)\left(1+\kappa^O_{24}\frac{M_n}{\mathcal{M}}\right), \tag{D14d}$$

$$V_{O,SO}(r) = -\frac{g^O_{13}g^O_{24}}{4\pi}\frac{8}{\sqrt{\pi}}\frac{m_O^5}{\mathcal{M}^4}\frac{m_O^2}{M_yM_n}\left[5-2m_O^2r^2\right]\exp(-m_O^2r^2)\cdot$$
$$\times\left\{3+\left(\kappa^O_{13}+\kappa^O_{24}\right)\frac{\sqrt{M_yM_n}}{\mathcal{M}}\right\}, \tag{D14e}$$

$$V_{O,Q}(r) = +\frac{g^O_{13}g^O_{24}}{4\pi}\frac{2}{\sqrt{\pi}}\frac{m_O^5}{\mathcal{M}^4}\frac{m_O^4}{M_y^2M_n^2}\left[7-2m_O^2r^2\right]\exp(-m_O^2r^2)\cdot$$
$$\times\left\{1+4\left(\kappa^O_{13}+\kappa^O_{24}\right)\frac{\sqrt{M_yM_n}}{\mathcal{M}}+8\kappa_{13}\kappa_{24}\frac{M_yM_n}{\mathcal{M}^2}\right\}, \tag{D14f}$$

$$V_{O,ASO}(r) = -\frac{g^O_{13}g^O_{24}}{4\pi}\frac{4}{\sqrt{\pi}}\frac{m_O^5}{\mathcal{M}^4}\frac{m_O^2}{M_yM_n}\left[5-2m_O^2r^2\right]\exp(-m_O^2r^2)\cdot$$
$$\times\left\{\frac{M_n^2-M_y^2}{M_yM_n}-4\left(\kappa^O_{24}-\kappa^O_{13}\right)\frac{\sqrt{M_yM_n}}{\mathcal{M}}\right\}. \tag{D14g}$$

3. Strange Meson-exchange

The rules for hypercharge nonzero exchange have been given in Ref. [38], see also [10]. The potentials for non-zero hypercharge exchange $(K, K^*, \kappa, K_A, K_B)$ are obtained from the expressions given in the previous subsections for non-strange mesons by taking care of the following points: (a) For strange meson exchange $\mathcal{P} = -\mathcal{P}_x\mathcal{P}_\sigma$. (b) In the latter case one has to replace both M_n and M_y by $\sqrt{M_yM_n}$, and reverse the sign of the antisymmetric spin orbit.

Appendix E: Additional One-Boson-Exchange QQ-Potentials

The extra vertices at the quark-level generate additional OBE-potentials. In the case of the vector mesons the extra vertex gives a change in the couplings

$$g_v \to g'_v = g_v - f_v \frac{\mathbf{k}^2}{4\mathcal{M}m_Q},\ f_v \to f'_v = f_v - f_v \frac{\mathbf{k}^2}{4m_Q^2},\ g_s \to g_s + g_s \frac{\mathbf{k}^2}{4m_Q^2}.$$

The extra vertices at the quark-level generate additional OBE-potentials. Neglecting the $\mathbf{k}^4$ etc terms we obtain the following contributions:

(a) Pseudoscalar-meson exchange: no additional potentials.

(b) Vector-meson exchange:

$$\begin{aligned}
\Delta\Omega_{1a}^{(V)} &= -\{g_{13}^v f_{24}^v + f_{13}^v g_{24}^v\}\,\frac{\mathbf{k}^2}{4\mathcal{M}m_Q},\ \ \Delta\Omega_{1b}^{(V)} = 0,\\
\Delta\Omega_{2a}^{(V)} &= -\frac{2}{3}\mathbf{k}^2\,\Delta\Omega_{3a}^{(V)} = 0,\ \ \Delta\Omega_{2b}^{(V)} = -\frac{2}{3}\mathbf{k}^2\,\Delta\Omega_{3b}^{(V)} = 0,\\
\Delta\Omega_{3a}^{(V)} &= -\left\{(g_{13}^v + f_{13}^v\frac{M_y}{\mathcal{M}})\,f_{24}^v\left(1+\frac{M_y}{m_Q}\right) + (g_{24}^v + f_{24}^v\frac{M_n}{\mathcal{M}})\,f_{13}^v\left(1+\frac{M_n}{m_Q}\right)\right\}\,\frac{\mathbf{k}^2}{4\mathcal{M}m_Q}/(4M_yM_n),\\
\Delta\Omega_{4}^{(V)} &= +\left\{\left(3+2\frac{\sqrt{M_yM_n}}{m_Q}\right)(g_{13}^v f_{24}^v + f_{13}^v g_{24}^v) + 4f_{13}^v f_{24}^v\frac{\sqrt{M_yM_n}}{\mathcal{M}}\right\}\left(\frac{\mathbf{k}^2}{4\mathcal{M}m_Q}\right)/(2M_yM_n),\\
\Delta\Omega_{5}^{(V)} &= +\left\{\left(1+4\frac{\sqrt{M_yM_n}}{m_Q}\right)(g_{13}^v f_{24}^v + f_{13}^v g_{24}^v) + 8f_{13}^v f_{24}^v\frac{\sqrt{M_yM_n}}{\mathcal{M}}\right\}\left(\frac{\mathbf{k}^2}{4\mathcal{M}m_Q}\right)/(16M_y^2M_n^2),\\
\Delta\Omega_{6}^{(V)} &= 0.
\end{aligned} \tag{E1}$$

(c) Scalar-meson exchange:

$$\begin{aligned}
\Delta\Omega_{1a}^{(S)} &= -g_{13}^s g_{24}^s\,\frac{\mathbf{k}^2}{2m_Q^2}\,,\ \Delta\Omega_{1b}^{(S)} = 0,\\
\Delta\Omega_{4}^{(S)} &= -g_{13}^s g_{24}^s\,\frac{\mathbf{k}^2}{4m_Q^2}\left[\frac{1}{M_yM_n}\right]\,,\ \Delta\Omega_{5}^{(S)} = g_{13}^s g_{24}^s\,\frac{\mathbf{k}^2}{4m_Q^2}\left[\frac{1}{8M_y^2M_n^2}\right],\\
\Delta\Omega_{6}^{(S)} &= -g_{13}^s g_{24}^s\,\frac{(M_n^2-M_y^2)}{4M_y^2M_n^2}\,\frac{\mathbf{k}^2}{2m_Q^2}.
\end{aligned} \tag{E2}$$

item[(d)] See below.

The transcription to configuration space potentials of these additional Pauli-invariants is similar to that in section D and is readily done. The results are

(a) Pseudoscalar-meson exchange: $\Delta V_P(r) = 0$.

(b) Vector-meson exchange:

$$\begin{aligned}\Delta V_V(r) \;=\; & \frac{m}{4\pi}\,\frac{m^2}{4\mathcal{M}m_Q}\Big[\left(g^v_{13}f^v_{24}+f^v_{13}g^v_{24}\right)\phi^1_C(r)\\
&-\frac{m^2}{6M_yM_n}\left\{\left(g^v_{13}+f^v_{13}\frac{M_y}{\mathcal{M}}\right)f^v_{24}\left(1+\frac{M_y}{m_Q}\right)+\left(g^v_{24}+f^v_{24}\frac{M_n}{\mathcal{M}}\right)f^v_{13}\left(1+\frac{M_n}{m_Q}\right)\right\}\phi^2_C(r)\,(\boldsymbol{\sigma}_1\cdot\boldsymbol{\sigma}_2)\\
&-\frac{m^2}{4M_yM_n}\left\{\left(g^v_{13}+f^v_{13}\frac{M_y}{\mathcal{M}}\right)f^v_{24}\left(1+\frac{M_y}{m_Q}\right)+\left(g^v_{24}+f^v_{24}\frac{M_n}{\mathcal{M}}\right)f^v_{13}\left(1+\frac{M_n}{m_Q}\right)\right\}\phi^1_T(r)\,S_{12}\\
&-\frac{m^2}{2M_yM_n}\left\{\left(3+2\frac{\sqrt{M_yM_n}}{m_Q}\right)(g^v_{13}f^v_{24}+f^v_{13}g^v_{24})+4f^v_{13}f^v_{24}\frac{\sqrt{M_yM_n}}{\mathcal{M}}\right\}\phi^1_{SO}(r)\,\mathbf{L}\cdot\mathbf{S}\\
&+\frac{m^4}{16M_y^2M_n^2}\left\{\left(1+4\frac{\sqrt{M_yM_n}}{m_Q}\right)\left(g^v_{13}f^v_{24}+f^v_{13}g^v_{24}\right)+8f^v_{13}f^v_{24}\frac{\sqrt{M_yM_n}}{\mathcal{M}}\right\}\frac{3}{(mr)^2}\,\phi^1_TQ_{12}\Big].\end{aligned}\tag{E3}$$

(b) Scalar-meson exchange:

$$\begin{aligned}\Delta V_S(r) \;=\; & -\frac{g^s_{13}g^s_{24}}{4\pi}\,\frac{m^3}{2m_Q^2}\left[\phi^1_C(r)+\frac{m^2}{2M_yM_n}\,\phi^1_{SO}(r)\,\mathbf{L}\cdot\mathbf{S}+\frac{m^4}{16M_y^2M_n^2}\frac{3}{(mr)^2}\,\phi^1_T\,Q_{12}\right.\\
&\left.+\frac{m^2}{M_yM_n}\left[\frac{(M_n^2-M_y^2)}{4M_yM_n}\right]\phi^1_{SO}\cdot\frac{1}{2}\,(\boldsymbol{\sigma}_1-\boldsymbol{\sigma}_2)\cdot\mathbf{L}\right].\end{aligned}\tag{E4}$$

(d) Axial-vector-meson exchange: The additional vertex for the axial-vector mesons is

$$\Delta\Gamma_\mu(p',p;k) \;=\; \frac{ig'_a}{\mathcal{M}^2}\varepsilon^{\mu\kappa\alpha\beta}\gamma_\kappa p'_\alpha p_\beta\tag{E5}$$

where we take $\mathcal{M}=M_N$. Restriction to terms of order $1/M_N^2$ the extra axial-vector exchange potential becomes

$$\begin{aligned}\Delta V_A(p',p) \;=\; & \frac{ig_ag'_a}{\mathcal{M}^2}\Big[[\bar u(p'_1,s'_1)u(p_1,s_1)]\,[\bar u(p'_2,s'_2)\gamma^\mu\gamma_5 u(p_2,s_2)]\,\varepsilon_{\mu\kappa\alpha\beta}\gamma_1^\kappa p_1'^\alpha p_1^\beta\\
&+[\bar u(p'_1,s'_1)\gamma^\mu\gamma_5 u(p_1,s_1)]\,[\bar u(p'_2,s'_2)u(p_2,s_2)]\,\varepsilon_{\mu\kappa\alpha\beta}\gamma_2^\kappa p_2'^\alpha p_2^\beta\Big]\,\left(\mathbf{k}^2+m_A^2\right)^{-1}\end{aligned}\tag{E6}$$

With Pauli-spinors this gives

$$\begin{aligned}\Delta V_A(p',p) \;=\; & -8\frac{g_ag'_a}{\mathcal{M}^2}\Big[\frac{i}{2}(\boldsymbol{\sigma}_1+\boldsymbol{\sigma}_2)\cdot\mathbf{q}\times\mathbf{k}-\frac{1}{4}\left(\boldsymbol{\sigma}_1\cdot\mathbf{k}\,\boldsymbol{\sigma}_2\cdot\mathbf{k}-\frac{1}{3}\mathbf{k}^2\,\boldsymbol{\sigma}_1\cdot\boldsymbol{\sigma}_2\right)\\
&-\frac{1}{6}\mathbf{k}^2\,\boldsymbol{\sigma}_1\cdot\boldsymbol{\sigma}_2\Big]\,\left(\mathbf{k}^2+m_A^2\right)^{-1}.\end{aligned}\tag{E7}$$

In configuration space this leads to

$$\Delta V_A(r) \;=\; -g_ag'_a\,\frac{m_A}{4\pi}\frac{m_A^2}{\mathcal{M}^2}\Big[8\phi^0_{SO}(r)\,\mathbf{L}\cdot\mathbf{S}+2\phi^0_T(r)\,S_{12}+\frac{4}{3}\phi^1_C(r)\,(\boldsymbol{\sigma}_1\cdot\boldsymbol{\sigma}_2)\Big]\tag{E8}$$

In order that folding with the nucleon wave function agrees in the 1/M expansion $g'_a=g_a$.

Remark: For the Quark-Nucleon additional potentials there is a factor 1/2. This because there is only an additional coupling in only one of the vertices of the Feynman-diagram.

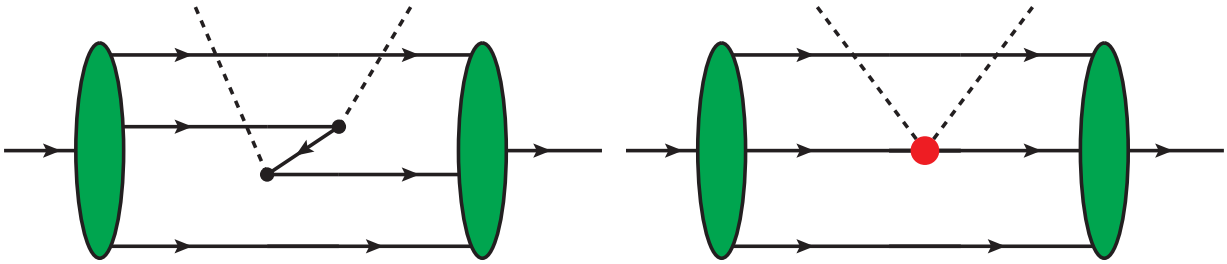

(a) Z-graph (b) Meson-pair Vertex

FIG. 8: Negative-energy quark contribution ⇒ MMQQ-coupling

Appendix F: Quarks and Meson-pairs

In the Nijmegen models it was in general assumed that negative-energy nucleons and hyperons are suppressed at low energies and nuclear densities. In ESC-models it is assumed that in principle the effects of the negative-energy baryons (Z-graph's) are eventually included effectively in the meson-pair couplings to the baryons. The same is assumed for the internal quark negative-energy states. This is illustrated in Fig. 8: the Z-graph (a) is included into the meson-meson-quark-quark (MMQQ) coupling. Then, assuming that the negative-energy contributions from the baryons are negligible we can suppose that the complete MPE in the baryonic nuclear force can be generated by relating the meson-pair coupling to the quarks from that to the baryons, similarly as is done in this paper for the meson-couplings to the quarks.

[1] Th.A. Rijken, *Constituent Quark model and NN-potentials* http://nn-online.org/eprints.
[2] Th.A. Rijken, *Nucleon-nucleon Interactions*, talk at the KITPC workshop on Present Status Nuclear Interaction Theory, Beijin August 2014.
[3] A. Le Yaouanc, L. Oliver, O. Péne, and J.-C. Raynal, Phys. Rev. D **8** (1973), 2223.
[4] O.W. Greenberg, Phys. Rev. Lett. **13** (1964), 598; J.J.J. Kokkedee, *The quark model*, W.A. Benjamin, New York, 1969.
[5] L. Micu, Nucl. Phys. B **10** (1969), 521; R. Carlitz and M. Kislinger, Phys. Rev. D **2** (1970), 336.
[6] A. Manohar and H. Georgi, Nucl. Phys. B **234** (1984), 189.
[7] A.A. Belavin, A.M. Polyakov, A.S. Schwarz, and Yu.S. Tyupkin, Phys. Lett. **59B** (1975), 85.
[8] D.I. Diakonov and V.Yu. Petrov, Nucl. Phys. B **272** (1986), 457-489.
[9] M.M. Nagels, Th.A. Rijken, and Y. Yamamoto, Phys. Rev. C **99** (2019), 044002.
[10] M.M. Nagels, Th.A. Rijken, and Y. Yamamoto, Phys. Rev. C **99** (2019), 044003.
[11] M.M. Nagels, Th.A. Rijken, and Y. Yamamoto, Phys. Rev. C **102** (2020), 054003.
[12] T.A. Rijken, Ann. Phys. (N.Y.) 164 (1985), 23.
[13] Th.A. Rijken, M.M. Nagels, and Y. Yamamoto, Progr. Theor. Phys. Suppl. **185** (2010), 14.
[14] V. G. Kadyshevsky, Sov. Phys. JETP, **19** (1964), 443.
[15] V. G. Kadyshevsky, Nucl. Phys. B **6** (1967), 125.
[16] V. G. Kadyshevsky and N. D. Mateev, Nuov. Cim. A **55** (1968), 275.
[17] C. Itzykson, V. G. Kadyshevsky, and I. T. Todorov, Phys. Rev. D **1**
[18] L.Ya. Glozman and D.O. Riska, Physics Reports, **268** (1996), 263-303.
[19] S. Weinberg, Phys. Rev. D **11** (1975), 3583.
[20] G. 't Hooft, Phys. Rev. D **14** (1976), 3432.
[21] D.I. Diakonov and V.Yu. Petrov, Phys. Lett. B **147** (1984), 351.
[22] D.I. Diakonov and V.Yu. Petrov, Nucl. Phys. B **245** (1984), 259-292.
[23] E.V. Shuryak, Phys. Rep. C **115** (1984), 152.
[24] E.V. Shuryak, Nucl. Phys. B **203** (1982), 93-115.
[25] M.A. Shiffman, A.I. Vainshtein, and V.I. Zakharov, Nucl. Phys. B **147** (1979), 385, 448.
[26] L.Ya. Glozman, e-print nucl-th/9909021 (1999).
[27] L.Ya. Glozman, W. Plessas, and K. Varga, Nucl. Phys. A **666 & 667** (2000), 29c-32c.
[28] Y. Nambu and G. Jona-Lasinio, Phys. Rev. **122** (1961), 345; *ibid* Phys. rev. **124** (1961) 246.
[29] D. Diakonov, in *Selected Topics in Non-perturbative QCD*, Proceedings of the Enrico Fermi School, Course CXXX, edited by A. DiGiacomo and D. Diakonov, Bologna (1996); arXiv:hep-ph-9602375.
[30] L.Ya. Glozman and K. Varga, Phys. Rev. D **61** (2000), 074008.
[31] H.A. Bethe and J. Goldstone, Proc. Roy. Soc. (London) A, **238** (1957), 551.
[32] H.A. Bethe, Ann. Rev. Nucl. Sci., **21** (1971), 93.
[33] Th.A. Rijken and J.W. Wagenaar, *Topics in Kadyshevsky Field Theory*, Report THEF-NIJM 09.07, http://nn-online.org/eprints
[34] Th.A. Rijken and J.W. Wagenaar, Progr. Theor. Phys. Suppl. **186** (2010), 282.
[35] Th.A. Rijken, Phys. Rev. C **73** (2006), 44007.
[36] Th.A. Rijken and Y. Yamamoto, Phys. Rev. C **73** (2006), 44008.
[37] Th. A. Rijken, Ann. Phys. (N.Y.) **208** (1991), 253.
[38] M.M. Nagels, Th.A. Rijken, and J.J. de Swart, Phys. Rev. D **15** (1977), 2547.
[39] M.M. Nagels, Th.A. Rijken, and J.J. de Swart, Phys. Rev. D **17** (1978), 768.
[40] P.M.M. Maessen, Th.A. Rijken, and J.J. de Swart, Phys. Rev. C **40** (1989), 2226.
[41] J.J. de Swart, M.M. Nagels, Th.A. Rijken, and P.A. Verhoeven, Springer Tracts in Modern Physics, Vol. **60** (1971), 138-203,
[42] At this point it is suitable to change the notation of the initial and final momenta. We use from now on the notations $\mathbf{p}_i \equiv \mathbf{p}$, $\mathbf{p}_f \equiv \mathbf{p}'$ for both on-shell and off-shell momenta.
[43] J.T. Brown, B.W. Downs, and C.K. Iddings, Ann. Phys. (N.Y.) **60** (1970), 148.
[44] C. Itzykson and J-B Zuber, *Quantum Field Theory*, McGraw-Hill Inc. (1980).
[45] N. Nakanishi, Suppl. Progr. Theor. Phys. **51** (1972), 1 .
[46] N. Nakanishi and I. Ojima, *Covariant Operator Formalism of Gauge Theories and quantum Gravity*, section 2.4.2, World Scientific Lecture Notes in Physics, Vol. 27, World Scientific Pub. Co., 1990.

[47] J.D. Bjorken and S.D. Drell, *I. Relativistic Quantum Mechanics* and *II. Relativistic Quantum Fields*, McGraw-Hill Publishing Company, 1965.
[48] Note that in this paper we suppose that f_A does not contain the one-pion-pole etc. In momentum space $\widetilde{f}_A(\mathbf{k}^2)$ is a smooth function of $\mathbf{k}^2$.
[49] H. Miyazawa, Phys. Rev. **104** (1956), 1741.
[50] J.-I. Fujita and H. Miyazawa, Progr. Theor. Phys. **17** (1957), 360.
[51] J.J. de Swart, Rev. Mod. Phys. **35** (1963), 916; *ibid.* **37** (1965), 326(E).
[52] P.A. Carruthers, *Introduction to unitary symmetry*, John Wiley & Sons Inc., New York (1966).
[53] Th.A. Rijken, V.G.J. Stoks, and Y. Yamamoto, Phys. Rev. C **59** (1999), 21.
[54] M. Hutter, *Instantons in QCD, Theory and Application of the Instanton Liquid Model*, Ph.D.-thesis, University of Munich, 1995.
[55] A. Rujula, H. Georgi, and S. Glashow, Phys. Rev. D **12** (1975), 147.
[56] J.E.F.T. Ribeiro, Z. Physik C, Particles and Fields **5** (1980), 27.
[57] L.Ya. Glozman, Z. Papp, W. Plessas, K. Varga, and R.F. Wagenbrunn, *Effective Q-Q interactions in constituent quark models*, arXiv:nucl-th/9705011 (1997); Phys. Rev. C **57** (1998), 3406; Phys. Rev. C **58** (1998), 094030.
[58] L.Ya. Glozman, Z. Papp, W. Plessas, Phys. Lett. B **381** (1996), 311.
[59] V.G.J. Stoks, R.A.M. Klomp, M.C.M. Rentmeester, and J.J. de Swart, Phys. Rev. C **48** (1993), 792.
[60] R.A.M. Klomp, private communication.
[61] R.A. Bryan and A. Gersten, Phys. Rev. D **6** (1972), 341.
[62] Th.A. Rijken and V.G.J. Stoks, Phys. Rev. C **54** (1996), 2869; ibid. Phys. Rev. C **54** (1996), 2869.
[63] M.M. Nagels, Th. Rijken, J.J. de Swart, G.C. Oades, J.L. Petersen, A.C. Irving, C. Jarskog, W. Pfeil, H. Pilkuhn, and H.P. Jacob, Nucl. Phys. B **147** (1979), 189-276.
[64] B. ter Haar and R. Malfliet, Physcics Reports, **149** (1987), 207-286.
[65] R. Brockmann and R. Machleidt, Phys. Rev. C **42** (1990), 1965.
[66] M. Baldo, I. Bombaci, L.S. Ferreira, G. Giansiracusa, and U. Lombardo, Phys. Rev. **43** (1991), 2605.
[67] G.F. Burgio, M. Baldo, P.K. Sahu, H.-J. Schulze, Phys. Rev. C **66** (2002), 025802.
[68] L.B. Okun, *Leptons and Quarks*, chapter 29, North-Holland Publishing Company (1984).